# Photoreceptors of *Nrl*$^{-/-}$ Mice Coexpress Functional S- and M-cone Opsins Having Distinct Inactivation Mechanisms

Sergei S. Nikonov,[1] Lauren L. Daniele,[1] Xuemei Zhu,[2] Cheryl M. Craft,[2] Anand Swaroop,[3] and Edward N. Pugh Jr.[1]

[1]F. M. Kirby Center for Molecular Ophthalmology, Department of Ophthalmology, School of Medicine, University of Pennsylvania, Philadelphia, PA 19104

[2]Mary D. Allen Laboratory for Vision Research, Doheny Eye Institute, and Department of Ophthalmology and Department of Cell and Neurobiology, Keck School of Medicine, University of Southern California, Los Angeles, CA 90033

[3]Department of Ophthalmology and Visual Sciences and Department of Human Genetics, University of Michigan, Ann Arbor, MI 48105

ABSTRACT The retinas of mice null for the neural retina leucine zipper transcription factor (*Nrl*$^{-/-}$) contain no rods but are populated instead with photoreceptors that on ultrastructural, histochemical, and molecular criteria appear cone like. To characterize these photoreceptors functionally, responses of single photoreceptors of *Nrl*$^{-/-}$ mice were recorded with suction pipettes at 35–37°C and compared with the responses of rods of WT mice. Recordings were made either in the conventional manner, with the outer segment (OS) drawn into the pipette ("OS in"), or in a novel configuration with a portion of the inner segment drawn in ("OS out"). *Nrl*$^{-/-}$ photoreceptor responses recorded in the OS-out configuration were much faster than those of WT rods: for dim-flash responses $t_{peak}$ = 91 ms vs. 215 ms; for saturating flashes, dominant recovery time constants, $\tau_D$ = 110 ms vs. 240 ms, respectively. *Nrl*$^{-/-}$ photoreceptors in the OS-in configuration had reduced amplification, sensitivity, and slowed recovery kinetics, but the recording configuration had no effect on rod response properties, suggesting *Nrl*$^{-/-}$ outer segments to be more susceptible to damage. Functional coexpression of two cone pigments in a single mammalian photoreceptor was established for the first time; the responses of every *Nrl*$^{-/-}$ cell were driven by both the short-wave (S, $\lambda_{max} \approx 360$ nm) and the mid-wave (M, $\lambda_{max} \approx 510$ nm) mouse cone pigment; the apparent ratio of coexpressed M-pigment varied from 1:1 to 1:3,000 in a manner reflecting a dorso-ventral retinal position gradient. The role of the G-protein receptor kinase Grk1 in cone pigment inactivation was investigated in recordings from *Nrl*$^{-/-}$/*Grk1*$^{-/-}$ photoreceptors. Dim-flash responses of cells driven by either the S- or the M-cone pigment were slowed 2.8-fold and 7.5-fold, respectively, in the absence of Grk1; the inactivation of the M-pigment response was much more seriously retarded. Thus, Grk1 is essential to normal inactivation of both S- and M-mouse cone opsins, but S-opsin has access to a relatively effective, Grk1-independent inactivation pathway.

KEY WORDS: phototransduction • GPCR signaling • cone opsin • Grk1 • spectral sensitivity

## INTRODUCTION

Healthy cone photoreceptor function is essential to normal human vision. The special importance of cones comes from at least three features of these cells: first, they initiate vision in the macula, the highly specialized central region of the retina whose signals map to a large portion of primary visual cortex; second, they provide the signals for color vision, allowing us to discriminate targets on the basis of their spectral content; third, they enable the retina to signal in the presence of strong ambient illumination (Burkhardt, 1994; Pugh et al., 1999; Paupoo et al., 2000).

Cone-specific disease, and disease of nearby rod and retinal pigment epithelium cells that lead to the demise of cones, have disastrous consequences for human vision (http://www.sph.uth.tmc.edu/Retnet/). More than 15 genes are currently known to be associated with autosomal dominant macular degeneration (http://www.sph.uth.tmc.edu/Retnet/); many more will certainly be discovered to be involved in age-related macular degeneration (Stone et al., 2004). To investigate the molecular mechanisms of cone disease, as well as the normal mechanisms that allow cones to perform their unique functions, it is critical to have mammalian models that allow (1) genomic analysis, and manipulation of genes expressed in cones; (2) molecular and biochemical characterization of the protein products of such genes; and (3) functional analysis of cones and their circuits. There is a striking paucity of such models when it comes to cones, and none yet that allow investigation on all three levels.

The mouse is increasingly the mammalian species of choice for the investigation of the functional properties

S.S. Nikonov and L.L. Daniele contributed equally to this work.
Correspondence to Edward N. Pugh Jr.: pugh@mail.med.upenn.edu

*Abbreviations used in this article:* OS, outer segment; WT, wild-type.


J. Gen. Physiol. © The Rockefeller University Press • 0022-1295/2005/03/287/18 $8.00
Volume 125 March 2005 287–304
http://www.jgp.org/cgi/doi/10.1085/jgp.200409208

of neuronal cell types and tissues, because of the advanced genomics, the array of tools available for its genetic manipulation, and the rapid generational time. In retinal research, definitive studies of the role of specific proteins in rod phototransduction (Xu et al., 1997; Chen et al., 1999, 2000; Mendez et al., 2000, 2001; Burns et al., 2002) and rod-based disease (for review see Pierce, 2001) have come from the genetic manipulation of rod photoreceptor-specific genes in mouse. However, in wild-type (WT) mice, cones constitute only ~3% of the photoreceptors, with rods comprising the remaining 97% (Carter-Dawson and LaVail, 1979), precluding ready isolation of cone-specific proteins in the large background of their rod homologues. Furthermore, mouse cones have few morphological features that would allow them to be distinguished from rods under the infrared viewing conditions required for single-cell photoreceptor electrophysiology. Thus, despite a few studies demonstrating cone-specific effects of photoreceptor-specific gene deletions in mouse with electroretinographic responses (Lyubarsky et al., 1999, 2000, 2001; Pennesi et al., 2003), the full-scale investigation of molecularly manipulated cone-specific genes has been an elusive goal.

The *Nrl* $^{-/-}$ mouse is a promising mouse model for the investigation of cone function. The developing *Nrl* $^{-/-}$ retina produces no rods (Mears et al., 2001); rather, it is populated with photoreceptors exhibiting ultrastructural, histochemical, molecular, and kinetic features that support the hypothesis that they are indeed cones (Daniele et al., 2005). Here we establish that the single cone photoreceptors of the *Nrl* $^{-/-}$ mouse can be characterized in detail with single-cell suction pipette recordings.

The coexpression of two visual pigments in single vertebrate cone photoreceptor cells conflicts with the requirement for distinct neural channels to encode spectral information; the capacity to discriminate lights on the basis of their spectral content is potentially diminished when both pigments drive transduction in a single cone. Nonetheless, immunohistochemical evidence shows that cones of many mammals coexpress both an S-pigment and an M/L-pigment, including rabbits, hamsters, guinea pigs, various strains of mice (Rohlich et al., 1994; Ahnelt, 1998; Applebury et al., 2000; Lukats et al., 2002), pigs (Hendrickson and Hicks, 2002), and humans, both fetal and, to a much less extent, adult (Xiao and Hendrickson, 2000; Cornish et al., 2004). While pigment coexpression in cones is incontrovertible, its functional consequences remain largely unstudied. Cone-driven ERG b-wave evidence is consistent with the hypothesis that both S- and M-pigments[1] drive phototransduction in mouse cones (Lyubarsky et al., 1999), but this latter evidence could be explained by convergence of signals from distinct cone classes onto proximal neurons. Thus, there is of yet no incontrovertible evidence that both coexpressed photopigments drive phototransduction in individual cones. *Nrl* $^{-/-}$ photoreceptors now permit for the first time the characterization of the physiological consequences of coexpression, allowing detection of coexpression levels of cone M-pigment relative to UV-pigment at ratios as low as 1:10,000. Finally, the presence of two mammalian cone pigments in the same photoreceptor cell make it possible for the first time to compare responses driven by one or the other, and to assess the dependence of the inactivation of the two cone pigments on Grk1, the only G-protein receptor kinase known to be expressed in mouse cones. By examining the responses of photoreceptors of *Nrl* $^{-/-}$*/Grk1* $^{-/-}$ mice, we have determined that Grk1 is involved in the inactivation of both pigments, but that the S-pigment appears to possess an effective, Grk1-independent mechanism.

## MATERIALS AND METHODS

### *Animals*

All experiments were performed in compliance with National Institutes of Health guidelines, as approved by the Institutional Animal Care and Use Committees of the University of Pennsylvania. *Nrl* $^{-/-}$ and *Rho* $^{-/-}$ mice were generated at the University of Michigan (Mears et al., 2001) and New England Medical Center (Lem et al., 1999), respectively. Animals used for recordings were born and maintained in controlled ambient illumination on a 12-h light/dark cycle, with an illumination level of 2–3 lux. *Nrl* $^{-/-}$*/Grk1* $^{-/-}$ double knockout mice were produced at the University of Southern California (Zhu et al., 2003) by crossing the *Nrl* $^{-/-}$ mice with *Grk1* $^{-/-}$ mice (Chen et al., 1999).

### *Histochemistry*

Mouse eyes were removed and placed into 4% paraformaldehyde for at least 24 h, followed by overnight incubation in 30% sucrose/PBS. Cryosections of 20-μm thickness were made from whole *Nrl* $^{-/-}$ mouse eyes, embedded in tissue freezing medium (Triangle Biomedical Sciences), and kept at −80°C. Frozen sections were first washed and then incubated with normal goat serum, followed by primary antibodies at 1:5,000 dilution in PBS containing 5% BSA, 0.1% sodium azide, and 0.1% Triton X-100. After washing, sections were incubated in secondary antibodies at ~1:300 dilution. The primary antibody was a rabbit polyclonal raised against residues 3–16 of the mouse M-opsin (Zhu et al., 2003). Secondary antibodies were goat anti-rabbit conjugated to FITC (Jackson ImmunoResearch Laboratories).

[1]The mouse genome contains the genes of two cone pigments, one from the shortwave sensitive class 1 (SWS1) homology group having $\lambda_{max}$ = 359 nm (Yokoyama et al., 1998), and a second from the long/midwave sensitive homology group (MWS/LWS) with $\lambda_{max}$ = 508 nm (Sun et al., 1997). The SWS1 group has $\lambda_{max}$s ranging from 358 to 425 nm and includes the human S-cone pigment, while the MWS/LWS group has $\lambda_{max}$s ranging from 508 to 611 nm and includes both the human M-cone and L-cone pigments (Yokoyama and Yokoyama, 2000; Ebrey and Koutalos, 2001). To reflect their homology group memberships, in this manuscript we will often refer to the mouse cone pigments with the generic labels "S-cone pigment" and "M-cone pigment." At other times, when the ultraviolet sensitivity of the mouse S-pigment is at issue, we will use the terminology "UV-cone pigment" to denote the mouse cone pigment with $\lambda_{max}$ = 359 nm.

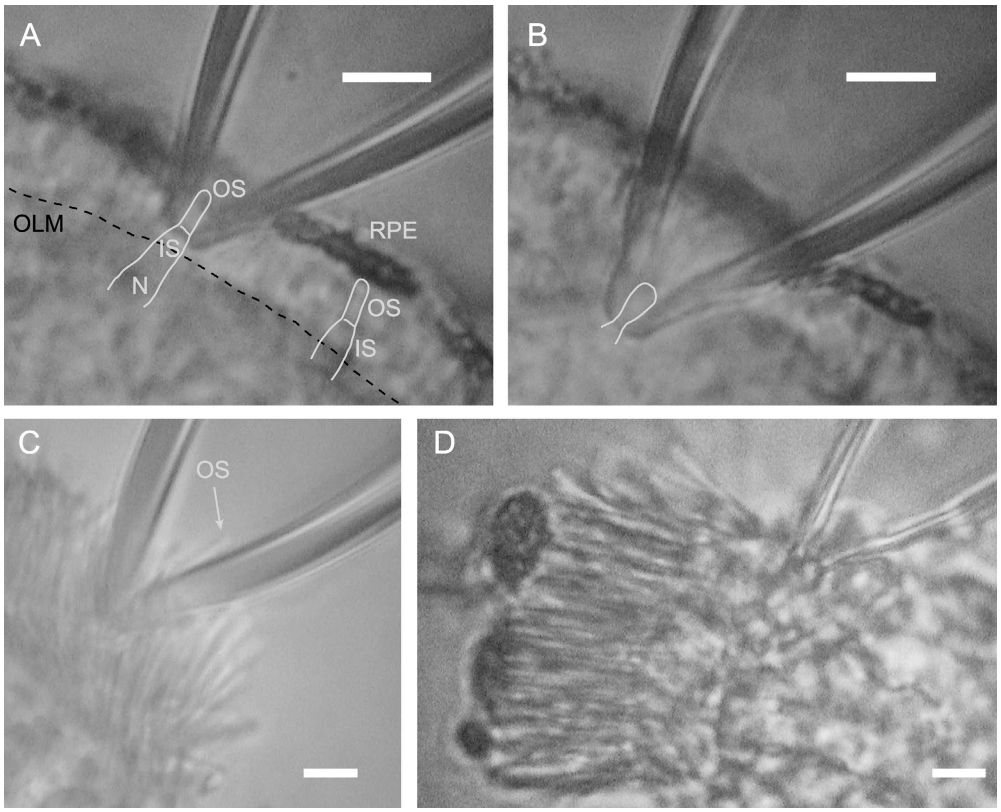


FIGURE 1. Illustration of two methods of "loose patch" recording from photoreceptors of the *Nrl*$^{-/-}$ (A and B) and WT (C and D) mouse retinas, imaged with infrared illumination ($\lambda > 1000$ nm). (A) Conventional "outer segment in" (OS in) method in which all or a portion of the outer segment is drawn into the suction pipette; the saturating photocurrent recorded in this case was 7 pA. Line drawings have been overlaid on the image to identify the key structures: OS, outer segment; IS, inner segment; N, nuclear region; RPE, retinal pigment epithelium; OLM, outer limiting membrane. At right one can see a array of refractive index variations perpendicular to the RPE layer that arise from the "palisade" of outer segments projecting into the RPE cell layer; one photoreceptor has been outlined on this array. Semithin plastic sections and high resolution EM images of the photoreceptor/RPE layers of the *Nrl*$^{-/-}$ retina (Daniele et al., 2005) have been used as a basis for the size and shape of the outlined cells; the images in this figure are blurred due to the limited resolution of infrared imaging. (B) OS-out method of recording in which the nuclear region of one (or more) cell is drawn into the suction pipette; in this case the saturating response was 9 pA, and data from this cell are included in the paper. The images of A and B are of the same retinal slice (though shifted in the chamber). (C) Image of WT retina with portion of rod outer segment drawn into the suction pipette (OS-in configuration); no recording was associated with this image, but the average amplitude of the saturating photocurrent in this configuration was 16 pA (Table I). (D) Image of WT retina with nuclear region of cells drawn into pipette; the saturating amplitude of the photocurrent was 34 pA, and it appeared that two nuclei had been drawn into the pipette. In each image the white bar represents 10 μm.

### *Tissue Preparation and Electrophysiological Methods*

Mice were killed, the eyes enucleated, and whole retinas removed from eye cups under infrared illumination. Small pieces of retina were dissected in a drop of chilled Locke's solution (112.5 mM NaCl, 3.6 mM KCl, 2.4 mM $MgCl_2$, 1.2 mM $CaCl_2$, 10 mM Hepes, 0.02 mM EDTA, 20 mM $NaHCO_3$, 3 mM $Na_2$-succinate, 0.5 mM Na-glutamate, 10 mM glucose), and placed into a recording chamber. The chamber was continuously refreshed with Locke's solution, pH 7.4, equilibrated with 95% $O_2$/5% $CO_2$, and maintained at 35–37°C with a heating system designed for microscopy (ALA Scientific). Using silanized suction pipettes, we recorded from photoreceptors embedded in 50–100-μm diameter slices of retina in either of two configurations, as we explain in the next section. In both recording configurations, once the tissue was drawn into the pipette, responses were evoked with calibrated flashes of light under control of a customized LabView (National Instruments Corp.) interface.

### *Novel Method of Suction Pipette Recording from the Perinuclear Region of Mouse Photoreceptors*

In our initial efforts to record from *Nrl*$^{-/-}$ photoreceptors, we employed the only method used to date for recording from mouse photoreceptors, drawing the outer segment into the suction pipette (e.g., Baylor et al., 1979b; Chen et al., 1995, 1999; Xu et al., 1997). However, we discovered (and report below) that the functional properties of *Nrl*$^{-/-}$ photoreceptors, unlike those of mouse rods, deteriorated during the recording epoch. These observations led us to develop a novel method of recording, in which a portion of the perinuclear region (broadly speaking, the "inner segment") of the photoceptor is drawn into the suction pipette (Fig. 1). A long history of suction pipette recordings from amphibian rods and cones has shown that essentially the same information can be obtained by recording from either segment (e.g., Cobbs and Pugh, 1987), as expected from the nature of the circulating current whose source is primarily $K^+$-selective current in the inner segment/nuclear region and whose sink is the outer segment cGMP-activated current (Hagins et al., 1970). However, mouse photoreceptors, unlike those of amphibians, are not readily isolated from one another, most likely because of much greater cell–cell adhesions in the outer nuclear layer and near the outer limiting membrane. We nonetheless found that very good recordings could be obtained with suction pipettes applied to thin retinal slices from which cells were not isolated, in effect using a "loose patch" configuration to record the portion of the overall circulating that flows through the perinuclear region (Fig. 1). To make the nomenclature of the recording methods

simple, we have named the new method "outer segment out" or "OS out" in contrast to the traditional "OS in" method. In the body of the paper we document the features of each type of recording.

### *Dissection to Obtain Tissue from Pieces of Retina of Known Location in Eye Coordinates*

To record from photoreceptors belonging to pieces of retina whose location of origin in the eye was known, a cautery (Aaron Medical Industries, Inc.) was used to mark the mid-dorsal and mid-nasal positions of each eye of a freshly killed mouse. Under infrared illumination on a dry surface of a Petri dish, each eye was trimmed of muscle tissue. A drop of superglue was placed nearby and the eye was lifted and gently placed onto the drop with the pupil oriented upwards. Two axis marks were made with a marker on the dish surface corresponding to mid-nasal and mid-dorsal positions, based on the visible cautery marks. After a few seconds, when the superglue was dry, the dish was filled with the Locke's solution. This procedure allowed for removal of the anterior segment without changing the eyecup's orientation. Pieces of retina of known topographic location (usually the most dorsal or ventral region; cf. Fig. 2) were then dissected from the eyecup and prepared for suction electrode recording as described above.

### *Light Stimulation and Calibration*

Flash stimulation was provided by two light sources, a tungsten halogen lamp, whose exposure duration was controlled by an electronic shutter (Uniblitz Model 222; Vincent Associates), and a xenon flash lamp that generates flashes of ~20 μs duration (Cobbs and Pugh, 1987). Flash intensity was varied by calibrated neutral density filters. Fully blocked interference filters with 10-nm bandwidth (FWHM transmittance) were used to produce monochromatic stimuli.

Flash energy densities were measured in photons $\mu m^{-2}$ at the image plane of the inverted microscope with calibrated photodiodes (United Detector Technology). The number of photoisomerizations per photoreceptor produced by a flash was estimated as the product of the energy density (photons $\mu m^{-2}$) and the outer segment collecting area, $a_c$ ($\mu m^2$), as described below.

### *Data Acquisition*

Data acquisition, stimulus timing, as well as control of neutral density and interference filters were under the control of a computer with a customized Labview interface (National Instruments Corp.). A current-to-voltage converter (model 8900; Dagan Corp.) was used to measure membrane photocurrents of outer segments; responses were filtered with a 4-pole lowpass filter with cutoff set to 30 Hz. Signals were digitized at 200 Hz with an A-D converter (National Instruments Corp.). Custom scripts written with Matlab software (Mathworks Corp.) were used to extract single trials from stored records, and to perform sorting, averaging, and other analyses.

### *Estimation of Light Collecting Area of WT Rods and Nrl $^{-/-}$ Photoreceptors*

The light collecting area of mouse photoreceptors illuminated transversely with unpolarized light in the recording chamber was estimated with the following formula:

$$a_C = 2.303 f \varepsilon_{max} \gamma C V_{OS} \times 10^{-4}, \quad (1)$$

where $f$ is a factor that depends on the polarization of the incident light relative to the plane of the disc membranes, $\varepsilon_{max}$ is the extinction coefficient at its $\lambda_{max}$ of the pigment in solution, $\gamma$ the quantum efficiency of photoisomerization, $C$ the concentration (M) of the pigment in the outer segment, and $V_{OS}$ ($\mu m^3$) the envelope volume of the outer segment, and the factor $10^{-4}$ is required for consistency with the dimensions of $V_{OS}$. This formula is essentially that of Baylor et al. (1979a), Eq. 20, except for the substitution of the product $f\varepsilon_{max}C$ for the specific pigment density.

*Collecting Area of Rods.* For WT mouse rods, we adopted the values $\varepsilon_{max}$ = 42,000 liter (mol cm)$^{-1}$ (Saari et al., 2001), $\gamma$ = 0.67, $C$ = 0.003 M, and $f$ = 3/4. The value $C$ = 0.003 M is derived from many microspectrophotometric (MSP) studies of rod and cone visual pigments in cells of larger diameter than mouse rods (Liebman, 1972), including "supersized" peripheral rods of some primates (Harosi, 1982). The average diameter and length of mouse rod outer segments are 1.4 and 23.6 μm, respectively (Carter-Dawson and LaVail, 1979), giving $V_{OS}$ = 37 $\mu m^3$. With all the parameters in Eq. 1 thus specified, the collecting area for a rod transversely illuminated in our recording chamber is estimated to be $a_c$ = 0.54 $\mu m^2$. The estimate $a_c$ = 0.48 $\mu m^2$ for mouse rods was provided in a recent investigation involving a similar experimental chamber (Calvert et al., 2001), and we thus adopted $a_c$ = 0.5 $\mu m^2$ as a reasonable compromise.

*Collecting Area of Nrl $^{-/-}$ Photoreceptors.* For *Nrl* $^{-/-}$ cells, we adopted the following values for the constants in Eq. 1: $\varepsilon_{max}$ = 41,670 liter (mol cm)$^{-1}$ (Vought et al., 1999), $\gamma$ = 0.67, and $C$ = 0.003 M (the value used for $\gamma$ is that widely accepted for mammalian rhodopsin, but we note that Okano et al. [1992] have estimated $\gamma$ = 0.61 and 0.62 for chicken cone rhodopsin and iodopsin, respectively). The pigment concentration in cones expressing a UV pigment has not been estimated with MSP, and almost certainly cannot be accurately measured in WT mouse cones or *Nrl* $^{-/-}$ photoreceptors due to their narrow width. However, quantitative immunoblot analysis of the total UV pigment content of the eye is consistent with a concentration equal to that of rods (Daniele et al., 2005). We assume $f$ = 3/4, as assumed for rods whose currents were recorded in the same configuration (above). Because experimenter selection might affect the length of the OS's of the cells from which we record electrically, we estimated the length of *Nrl*$^{-/-}$ outer segments from confocal images of pieces of live retina prepared in the same manner as for our physiological experiments, but incubated with the permeant fluorescent dye Calcein AM (Molecular Probes). This method gave abundant images of *Nrl* $^{-/-}$ outer segments resembling those seen under infrared illumination during physiological experiments. Outer segments in these confocal images had length 7.1 ± 0.2 μm (mean ± SEM, $n$ = 42; unpublished data), indistinguishable from the length, 7.3 ± 0.3 μm, measured with EM (Daniele et al., 2005). The average OS volume estimated from the EM data is $V_{OS}$ = 8.3 $\mu m^3$. With all parameters in Eq. 1 thus specified, we obtain $a_C$ = 0.11 $\mu m^2$ for the *Nrl*$^{-/-}$ outer segments in our experimental conditions. We assumed the photoreceptors of *Rho*$^{-/-}$ mice to have the same collecting area as those of the *Nrl*$^{-/-}$, based on the similarity of their appearance under recording conditions. We took this parallel approach to estimating $a_C$ of rods of WT mice, and of *Nrl*$^{-/-}$ and *Rho*$^{-/-}$ photoreceptors in order to make comparisons of the relative flash sensitivities and amplifications of the photoreceptor classes in the units of photoisomerizations/flash at $\lambda_{max}$, an approach that allows a comparison of the underlying transduction mechanisms in units intrinsic to photoreceptor function.

### *Quantitative Analysis of Response Data*

The activation phase of families of normalized responses $R(t)$ were fitted with a model of the phototransduction cascade (Lamb and Pugh, 1992; Pugh and Lamb, 1993),

$$R(t) \equiv \frac{r(t)}{r_{max}} = 1 - \exp[-1/2\Phi A(t - t_{eff})^2]. \quad (2)$$

In Eq. 2, "≡" signifies a definition, $r(t)$ is the photoresponse, $r_{max}$ its saturating amplitude, $\Phi$ the number of photoisomerizations produced by the flash, and $t_{eff}$ a brief (several ms) delay. Traces computed with Eq. 2 were convolved with digital filters to incorporate the effect of the membrane time constants of rods and cones (Smith and Lamb, 1997), set to $\tau_m$ = 1 or 5 ms, respectively, and the measured impulse response function of the analogue filter.

Amplitude vs. intensity functions were derived from response families and fitted with hyperbolic saturation functions of the form

$$R(t_{peak}) = \frac{r(t_{peak})}{r_{max}} = \frac{Q}{Q + Q_{1/2}}, \quad (3)$$

where $r(t_{peak})$ is the amplitude at the time to peak, $t_{peak}$, of the response, $Q$ is the flash intensity in photons $\mu m^{-2}$, and $Q_{1/2}$ the half-saturating intensity. With the amplitude–intensity function expressed in these units, the flash sensitivity $S_F$ of the normalized response is $S_F = 1/Q_{1/2}$.

## RESULTS

### *M-opsin Is Expressed in a Dorso-ventral Gradient in the Nrl$^{-/-}$ Retina*

As revealed with immunohistochemistry, rodent retinas typically express two cone visual pigments, an S-opsin and an M-opsin, and most rodents are known to co-express these opsins in at least some of their cones (Rohlich et al., 1994; Applebury et al., 2000). Therefore, we investigated the extent of M-cone pigment expression in the *Nrl*$^{-/-}$ retina with immunolabeling. A clear dorso-ventral gradient of labeling is observed (Fig. 2). Comparisons of immunolabeled cells with concurrently taken DIC images indicated that most photoreceptors express M opsin at a level that can be detected with immunolabeling (unpublished data). Our physiological experiments (described below) reveal both mouse UV-cone opsin and M-cone opsin to be present in each *Nrl*$^{-/-}$ photoreceptor from which we have recorded and, further, allowed quantitative assessment of the relative levels of expression of M- and UV-opsin in single cells.

### *The Response Kinetics of Nrl$^{-/-}$ Photoreceptors Are Faster than Those of WT Rods*

As benchmarks for comparison with *Nrl*$^{-/-}$ photoreceptors we made parallel recordings of rods from WT mice (Fig. 3). In our initial experiments we recorded from both types of photoreceptors, and from a small population of cones of the *Rho*$^{-/-}$ mouse, in the traditional configuration used for mouse rods (e.g., Xu et al., 1997), drawing the outer segment into the suction electrode ("OS in"; Fig. 3, A and G). However, we found that the responses of the *Nrl*$^{-/-}$ photoreceptors in the OS-in configuration changed over time (as described below), and so we developed a novel method (not previously used for recording from murine photoreceptors) in which a portion of the inner segment was drawn into the suction electrode (OS-out configuration, Fig. 3, D and J; cf. MATERIALS AND METHODS, Fig. 1). The response properties of *Nrl*$^{-/-}$ photoreceptors were strikingly different in the two configurations, while those of WT rods were quite similar. The latter similarity was expected from the long history of recordings from amphibian rods and cones, which have revealed the kinetics of circulating current suppression to

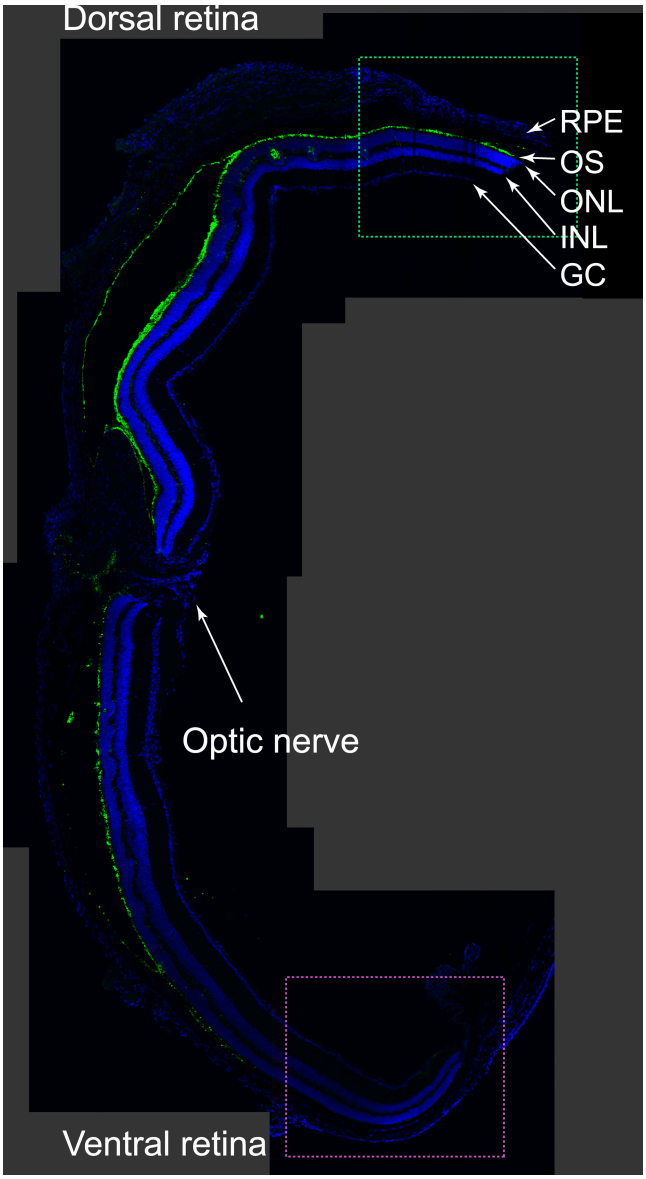


FIGURE 2. Dorso-ventral gradient of M-opsin expression in the *Nrl*$^{-/-}$ retina. Image shows a montage of a series of confocal scans from a single transverse section of a 3-mo-old mouse labeled with polyclonal rabbit anti-mouse M-opsin antibody (green) and mounted with a DAPI-containing mounting medium (blue) to show nuclei of the cells in different layers. The dashed boxes around dorsal and ventral portions of the retina illustrate the approximate retinal locations from which retinal slices were taken for the experiments described in Figs. 5 and 6.

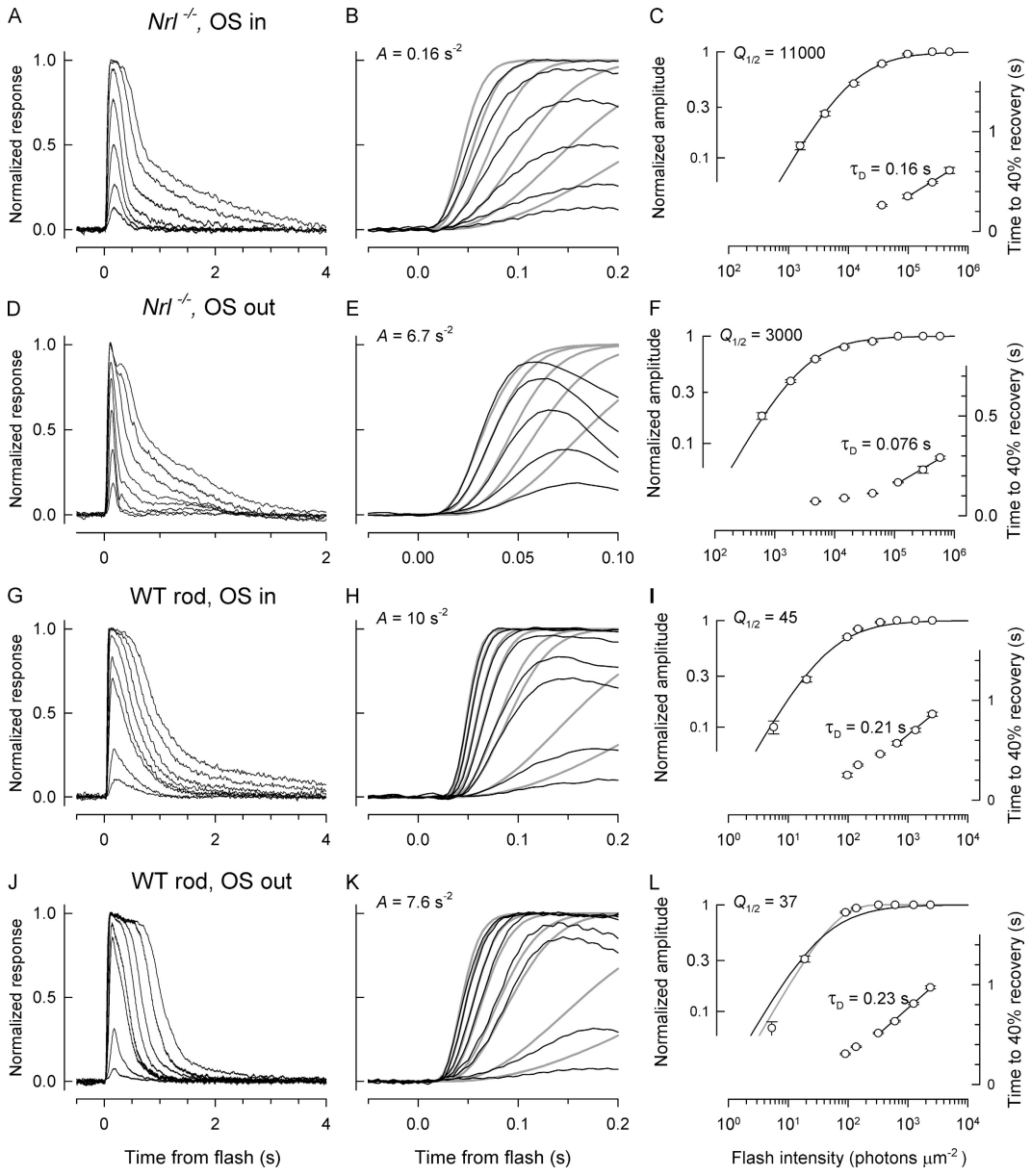


FIGURE 3. Comparison of the kinetics and sensitivity of responses of $Nrl^{-/-}$ and WT rod photoreceptors recorded in two configurations. Rods were stimulated with 501-nm flashes, while the $Nrl^{-/-}$ cells were stimulated with 361-nm flashes. Each row of panels presents data from one photoreceptor, recorded in one of two recording configurations described in Fig. 1. A, D, G, and J are light response families, while B, E, H, and K present the activation phases of the corresponding response family on a faster time base, with the traces fitted with the G-protein cascade model (smooth gray traces; cf. MATERIALS AND METHODS, Eq. 2); the corresponding amplification constants are given in the figures. C, F, I, and L plot the amplitude vs. intensity functions derived from the response family in the same row (left ordinate) and plot the time to 40% recovery (right ordinate) for responses to the intensities specified by the abscissa. The amplitude vs. intensity functions have been fitted with hyperbolic saturation functions (Eq. 3), whose half-saturation magnitudes, $Q_{1/2}$, are given in the figures. The recovery time points to the lowermost saturating intensities have been fitted in semilog coordinates ("Pepperberg plots") with a straight line to obtain the rate of increase in recovery time per e-fold change in intensity, which estimates $\tau_D$, the dominant recovery time constant (Pepperberg et al., 1994; Nikonov et al., 1998). All responses were filtered during acquisition with a 4-pole low pass analogue filter set at 30 Hz and digitized at 200 Hz. At least three responses to the same flash intensity were averaged for each trace, and at least 10 individual records were used to obtain the averaged responses to the dimmest flashes. The saturating photocurrent amplitudes were 26 pA ($Nrl^{-/-}$ cell, OS in), 10 pA ($Nrl^{-/-}$ cell, OS out), 26 pA (rod, OS in), 13 pA (rod, OS out). Note that the results in D and E are presented on a twofold shorter time scale than in the other panels.

be very similar, regardless of the segment in the pipette (e.g., Cobbs and Pugh, 1987). In contrast to WT rods, however, $Nrl^{-/-}$ photoreceptors in the OS-in configuration had reduced amplification, slower times to peak, somewhat increased dominant time constants of recovery, and were overall less sensitive to light than in the

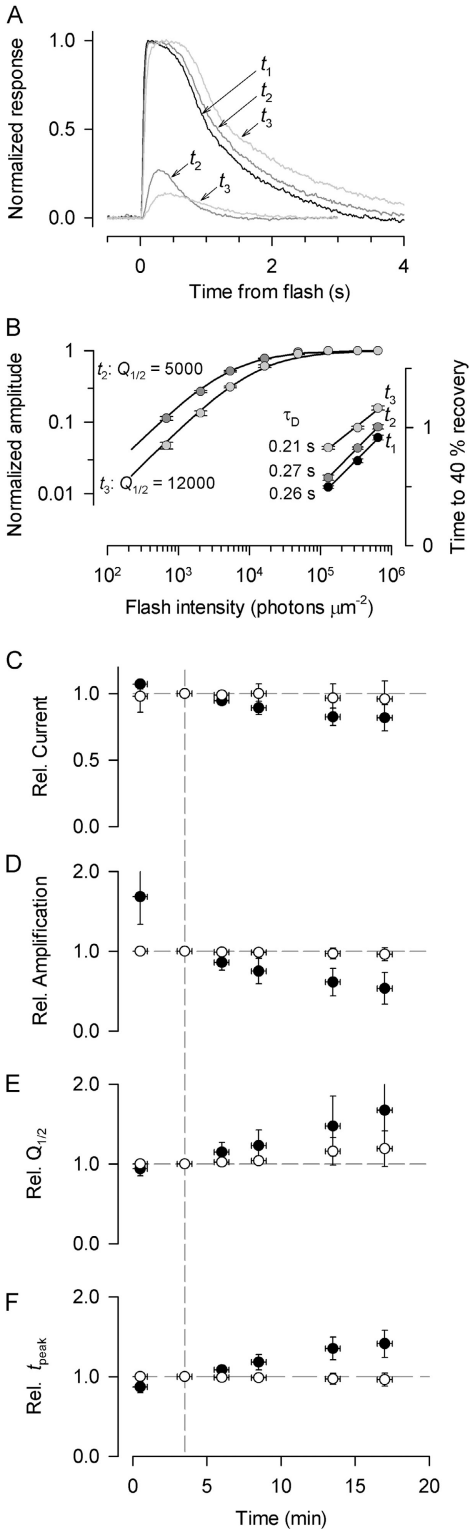


FIGURE 4. Relative stability of the response properties of *Nrl*$^{-/-}$ photoreceptors. (A) Traces show responses of a single *Nrl*$^{-/-}$ cell to dim (2,100 photons μm$^{-2}$) and bright (650,000 photons μm$^{-2}$) flashes of 361 nm at three different times during a 15-min recording epoch: $t_1$, the 1st min of recording; $t_2$, the 2nd to 5th min; $t_3$, the 15th min; responses got progressively slower and less sensitive. Note that dim-flash responses were not recording in the $t_1$ time frame. (B) Amplitude vs. intensity functions and "Pepperberg plots" for the cell of panel A at various times in the recording session ($t_i$ refers to the same period as in A). At about $t_2$, the half-saturating flash intensity, $Q_{1/2}$, was 5,000 photons μm$^{-2}$, but as the cell became less sensitive, $Q_{1/2}$ shifted to 12,000. The dominant recovery time constant $\tau_D$ was estimated as in the experiments of Fig. 1, and found to change little over the time course of the experiment. (C–F) Properties of the responses of 21 *Nrl*$^{-/-}$ cells (OS in, ●) and 8 *Nrl*$^{-/-}$ cells (OS out, ○) plotted as a function of time; the data of each cell was scaled relative to its values at ~3 min (dashed line), and then the data of each scaled population dataset averaged to produce the plotted points. The minimum number of records averaged for the first time point was 8 (OS in) and 2 (OS out), while for all other time points the number of records averaged ranged from 21 to 8 for cells in the two configurations, respectively. Horizontal bars give the time bracket of data extraction from the raw records; vertical error bars are 95% confidence intervals. The amplification of phototransduction, characterized by the coefficient *A* (D), declined very rapidly for *Nrl*$^{-/-}$ cells recorded in the OS-in configuration, and its value early in the recording epoch was estimated from a limited number of flashes rather than from complete response families.

OS-out configuration (Fig. 3; Table I). More importantly, in the OS-out configuration, *Nrl*$^{-/-}$ photoreceptors were reliably faster than rods, based on two criteria: first, the time to peak of the dim-flash response; second, the dominant time constant of recovery (Table I).

### *Relative Stability of Cells Recorded in OS-in and OS-out Configurations*

As the characterization of the responses of cells with series of flashes depends on their stability, we felt it critical to document the key properties of individual cells over the time epochs of the experiments (Fig. 4). To combine results obtained from different cells, we scaled the various response properties relative to their value at ~3 min (Fig. 4, C–F, vertical dashed line), an early time when data collection was typically in full swing. When recorded in the OS-in configuration, the circulating current of *Nrl*$^{-/-}$ photoreceptors declined slowly over the recording epoch (Fig. 4 C, ●), but the relatively small magnitude of the decline indicates that the electrochemical gradients of the cells were not seriously compromised over a 20-min recording session. Over the same epoch, however, the responses of cells in the OS-in configuration became markedly slower (Fig. 4, A and F), and progressively less sensitive to light (Fig. 4, B and E). In contrast, all the properties of the responses of *Nrl*$^{-/-}$ photoreceptors recorded in the OS-out configuration were quite stable (Fig. 4, C–F, ○). WT rods were completely stable in both configurations, for recording epochs of up to 2 h (unpublished data). Of particular note in the characterization of cells in the OS-in configuration is the decline in the initial acceleration of the response, captured in the amplification coefficient (Fig. 4 D); analysis of responses of a limited number of cells in the first two minutes of recording

TABLE I

*Comparison of Properties of Nrl $^{-/-}$, Rho$^{-/-}$, and WT Rod Photoreceptors of the Mouse*

| Genotype (configuration) (no. of cells) | $V_{OS}$ | $a_C$ | $R_{max}$ | $\tilde{S}_F$ | $A$ | $t_{peak}$ | $\tau_D$ |
|---|---|---|---|---|---|---|---|
| | $\mu m^3$ | $\mu m^2$ | $pA$ | $(\Delta R/\Phi)$ % | $s^{-2}$ | $ms$ | $ms$ |
| *Nrl* $^{-/-}$ (OS out, $n = 8$) | 8.3 | 0.11 | 13 ± 5 | 0.24 ± 0.06 | 3.5 ± 1.4 | 91 ± 6 | 110 ± 40 |
| *Nrl* $^{-/-}$ (OS in, $n = 30$) | 8.3 | 0.11 | 16 ± 3 | 0.23 ± 0.07 | 0.56 ± 0.21 | 200 ± 20 | 200 ± 20 |
| *Rho*$^{-/-}$ (OS in, $n = 8$) | 8.3 | 0.11 | 6 ± 1 | 0.08 ± 0.04 | 0.11 ± 0.07 | 250 ± 60 | 270 ± 50 |
| WT rods (OS out, $n = 10$) | 37 | 0.5 | 22 ± 8 | 5.1 ± 1.8 | 7.6 ± 1.4 | 200 ± 20 | 260 ± 60 |
| WT rods (OS in, $n = 13$) | 37 | 0.5 | 16 ± 4 | 5.6 ± 0.8 | 8.4 ± 1.4 | 210 ± 10 | 210 ± 40 |
| WT rods (all, $n = 23$) | 37 | 0.5 | – | 5.3 ± 1.0 | 8.0 ± 1.0 | 207 ± 9 | 230 ± 20 |

Columns 2–8 present parameters of the cells whose type is identified in the first column: $V_{OS}$ is the envelope volume of the outer segment, $a_C$ the light collecting area (MATERIALS AND METHODS), $R_{max}$ the saturating amplitude of the light response, $\tilde{S}_F$ the sensitivity of the normalized dim flash response, specified as fraction of the saturating response per photoisomerization ($\Delta R/\Phi$) (cf. Eq. 3), $A$ the amplification constant (Pugh and Lamb, 1993), $t_{peak}$ the time to peak of the dim-flash response, and $\tau_D$ the dominant recovery time constant (cf. Fig. 3). The error terms are 95% confidence intervals; the number of cells of each type is given with the genotype specification. The results in the table are based on recordings made 2–6 min after recording commenced (except for rods, and *Nrl* $^{-/-}$ cells in the OS-out configuration, for which the recordings were stable for long epochs; cf. Fig. 4). In the bottom row, the weighted average of the results from all the rods are provided, as none of the functional properties (with the exception of $R_{max}$) differed between rods recorded in the two configurations with statistical reliability; $R_{max}$ can be expected to differ, as nothing insures that the perinuclear region drawn into the suction pipette in the OS-out configuration contains all of the $K^+$-selective channels that constitute the "inner segment" limb of the circulating current.

indicated that amplification declined rapidly at early times, eventually reaching a value at 20 min that on average was more than sixfold lower in the OS-in as compared with the OS-out configuration (Table I). Two nonmutually exclusive explanations of the lability of the *Nrl* $^{-/-}$ photoreceptors in the OS-in configuration are that the outer segments of these cells are more vulnerable than rods to physical damage by the suction pipette, and/or that the cone-like disc membranes are more susceptible to some other compromising alteration when removed from their extracellular matrix sheath (Daniele et al., 2005; cf. DISCUSSION).

### *S- and M-opsins Are Coexpressed and Functional in Nrl $^{-/-}$ and Rho$^{-/-}$ Photoreceptors*

Immunohistochemistry presented here (Fig. 2) suggests that many, if not all, of the *Nrl* $^{-/-}$ photoreceptors coexpress S- and M-cone opsins in a dorso-ventral gradient, as do the cones of three strains of mice (Applebury et al., 2000), and other rodents (Rohlich et al., 1994; Dkhissi-Benyahya et al., 2001; Lukats et al., 2002). It is not yet known, however, if the coexpressed pigments are both functional in individual cells, i.e., both capable of activating phototransduction in the same cell. To further investigate this issue, we measured the spectral sensitivities of single *Nrl* $^{-/-}$ photoreceptors. After an initial response family to 361-nm flashes was measured, cells were presented with sets of flashes of test wavelengths ranging from 361 to 690 nm, interleaved with 361-nm standards, and periodic intense flashes to determine the magnitude of the saturating current. Sensitivity at each wavelength was determined as described above (Eq. 3; cf. Fig. 3, C and F); in each case normalized at 361 nm. The data of one *Nrl* $^{-/-}$ cell for which sensitivity was measured at 10 different wavelengths (Fig. 5 A, ▲) shows that the spectrum of an individual cell can be described with a pair of pigment template curves characteristic of the mouse UV- and M-cone pigments. Similar results were obtained from a number of cells. Spectral sensitivities measured in this manner revealed that every *Nrl* $^{-/-}$ photoreceptor recorded functionally coexpressed both UV and M-opsin (Fig. 5 B). All *Nrl* $^{-/-}$ cells were maximally sensitive at ~360 nm, but above ~440 nm the sensitivity did not track the UV-cone pigment template (Fig. 5, purple curves). For simplicity, we present in Fig. 5 B the sensitivities of 36 *Nrl* $^{-/-}$ cells and 8 *Rho*$^{-/-}$ cells at just three wavelengths, 361 nm, and at either 501 or 515 nm. The relative sensitivity at the middle wavelengths varied >1,000-fold over the population. Nonetheless, even the cells least sensitive at 501 or 515 nm were 20-fold more sensitive than would be expected if they expressed only the UV-pigment (Fig. 5 B, gray arrow).

We measured the spectral sensitivity of rods (Fig. 5 A) as a benchmark for the spectra of the *Nrl* $^{-/-}$ photoreceptors. The rod data are well described over a spectral range of 250 nm and nearly five log units of sensitivity by a pigment template (Lamb, 1995), modified to include the sensitivity of the pigment β-band (Govardovskii et al., 2000) (Fig. 5 A, black curve), providing assurance that the spectra of the cells of the knockout mice have been accurately measured. Spectral sensitivities of rods recorded in the OS-in and OS-out configuration were indistinguishable, showing that the pipette does not distort the spectrum.

An important question is whether the large variation in coexpression of the M-pigment manifest in the spectral sensitivity near 510 nm reflects the dorso-ventral gra-

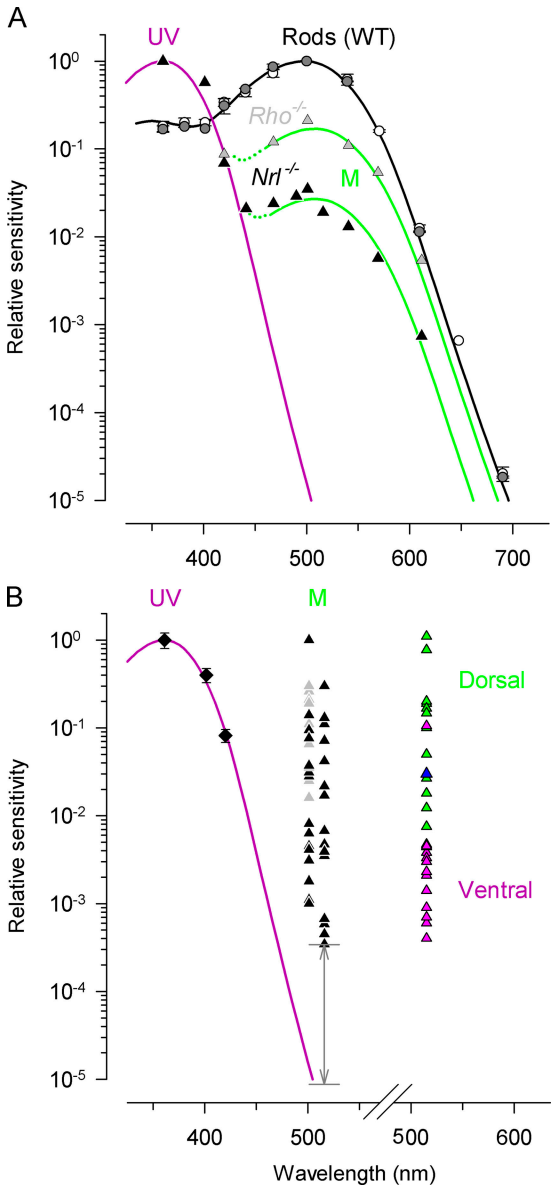


FIGURE 5. Spectral sensitivities of single mouse photoreceptors. The sensitivity of the cells of *Nrl*$^{-/-}$ and *Rho*$^{-/-}$ mice were normalized to unity at 361 nm, while rod sensitivities were normalized at 500 nm. (A) Data from a single *Nrl*$^{-/-}$ cell stimulated at 11 different wavelengths (▲) and data from a *Rho*$^{-/-}$ cell stimulated at 7 different wavelengths (gray triangle); both cells were recorded in the OS-in configuration. Averaged spectral sensitivities of seven rods (OS in, ○), and 2 rods (OS out, gray circle); error bars are standard deviations. The unbroken curves are pigment templates (Lamb, 1995) for the three murine pigments: $\lambda_{max}$ = 361 nm (purple curve; UV-cone pigment), $\lambda_{max}$ = 508 nm (green curve; M-cone pigment), and $\lambda_{max}$ = 500 nm (black; rhodopsin; for $\lambda <$ 450 nm the rhodopsin template was extended into the short-wave region of the pigment β-band according to Govardovskii et al. (2000). Dotted traces are the sum of M-pigment templates and UV-pigment template. (B) Results from 9 *Nrl*$^{-/-}$ cells stimulated with 361, 401, and 420-nm flashes (◆); error bars are 95% confidence intervals. Results from 36 different *Nrl*$^{-/-}$ cells stimulated with 361-nm and 501 or 515-nm flashes (▲), and from 8 *Rho*$^{-/-}$ cells (gray triangle). The gray arrow indicates the gap between the measured sensitivity of the *Nrl*$^{-/-}$ cells least sensitive at ~510 nm and the predicted sensitivity of a cell expressing only the UV-cone pigment (violet curve). Data points plotted to the right of the abscissa break show sensitivity measured at 515 nm for 12 *Nrl*$^{-/-}$ cells from the dorsal part of the retina (green triangle), one cell from the central part of the retina (blue triangle) and 12 cells from the ventral part of the retina (pink triangle). All results for this analysis were recorded in the OS-in configuration.

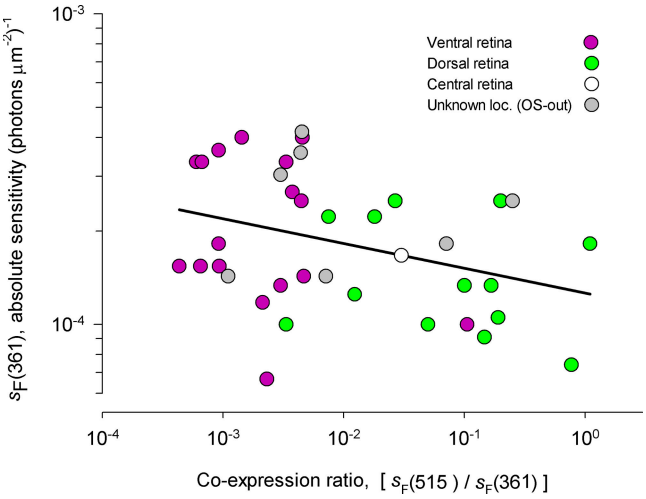


FIGURE 6. M-cone pigment coexpression in *Nrl*$^{-/-}$ photoreceptors affects the absolute sensitivity to stimuli detected by the UV-cone pigment. Each point in the plot represents data from a single *Nrl*$^{-/-}$ photoreceptor; the purple circles represent data from cells in slices from the most ventral portion of the retina, while the green circles represent data from cells in slices from the most dorsal portion of the retina, and the white circle one cell from a slice near the optic disc (see Fig. 2, colored boxes); these cells were recorded from in the OS-in configuration in a simplified protocol that focused only on the dim-flash responses. The gray circles plot data from cells recorded from in the OS-out configuration, in slices from unknown retinal locations. The abscissa plots the "co-expression ratio," defined as the ratio of the sensitivities ($s_F$) to dim flashes of 515 and 361-nm stimulation; the ordinate plots the absolute sensitivity to 361-nm stimulation, $s_F(361)$. The black line was determined from Pearson product-moment correlation analysis of the bivariate data: its slope is −0.08 $\log_{10}$ units of $s_F(361)$ per $\log_{10}$ units of the coexpression ratio; the slope is significantly different from zero ($t_{df=36} = -2.27$, $P < 0.02$).

dient seen in Fig. 2. To address this question, we measured the spectral sensitivity of photoreceptors from the most dorsal and most ventral portions of the retina (Fig. 5 B; cf. Fig. 2); the coexpression of M-pigment in cells from the dorsal retina was on average almost 100-fold greater than in cells from the ventral retina. However, there was also substantial variation in the degree of co-expression in the dorsal and ventral retina areas probed.

### *Coexpression of M-pigment Is Correlated with Reduced Absolute Sensitivity of the UV-pigment–driven Response*

The dorso-ventral gradient of M-pigment coexpression suggests that at least the M-cone pigment level is under

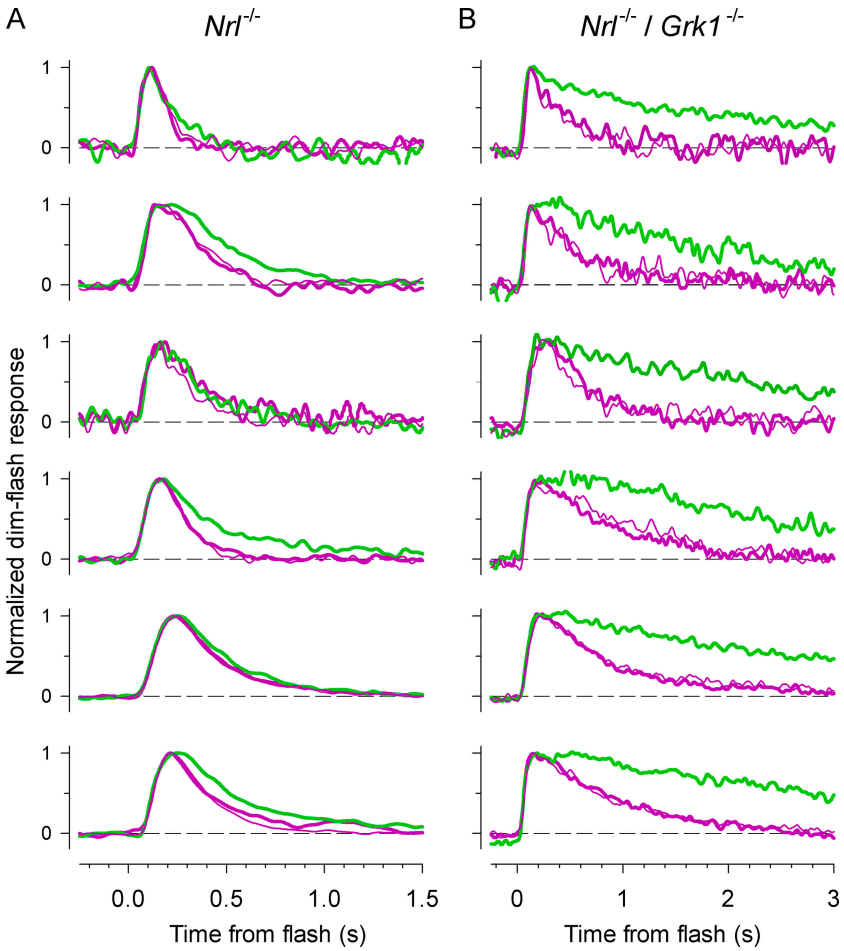


FIGURE 7. Dim-flash responses of individual photoreceptors from *Nrl* $^{-/-}$ mice (A) or *Nrl* $^{-/-}$*/Grk1*$^{-/-}$ mice (B) driven by either the UV-cone pigment (purple traces) or the M-cone pigment (green). Each panel presents averaged responses of a different single cell in response to a 361-nm flash (purple traces) and a 501 or 515-nm flash (green traces). In each experiment, the thicker purple trace was obtained first, then the green trace, and finally the thinner purple trace. The average number of responses taken for each trace was 31 (range, 10–70). The fraction of current suppressed by the flashes was 0.20 ± 0.11 (mean ± SD taken over the population) of the maximum, and did not differ for the responses to the UV and midwave flashes. Each trace is scaled to unity at its peak.

the regulation of a factor that varies in a dorso-ventral manner. We examined the hypothesis that the UV-cone pigment might also be regulated in a dorso-ventral gradient, but in an "inverse" manner to that of the M-pigment. We plotted the absolute sensitivity of *Nrl* $^{-/-}$ photoreceptors to 361-nm flashes as a function of the "coexpression ratio," defined as $s_F(515)/s_F(361)$, the ratio of sensitivity to 515-nm flashes relative to the sensitivity to 361-nm flashes (Fig. 6). There is a reliable negative correlation between $\log_{10}[s_F(361)]$ and $\log_{10}[s_F(515)/s_F(361)]$, with cells from the ventral retina having a higher absolute sensitivity to UV light. Interpreting the sensitivities as surrogates for the pigment expression levels, this result suggests that UV-cone pigment expression is down-regulated in cones in the regions of the retina where the M-pigment is up-regulated, and vice versa. In absolute terms, the effect is not large; thus, the sensitivity to UV light only declines (on average) about twofold over the nearly 3.5 $\log_{10}$ domain of coexpression. That the negative correlation is manifest on a 3,000-fold scale of coexpression indicates the that underlying regulatory mechanisms do not simply act to conserve the total amount of pigment; for example, this mechanism apparently exerts an influence on UV-pigment expression level even when M-pigment levels are 1/1,000 to 1/100 that of the UV-pigment.

### *Phototransduction Activated by the UV- and M-cone Opsins in Single Cells Is Similar*

The spectral sensitivity data establish that both UV- and M-cone photopigments are expressed in individual *Nrl* $^{-/-}$ and *Rho*$^{-/-}$ photoreceptors, and that both pigments can activate transduction in the same cell. Because the sensitivity in the midwave spectral region is far greater than would be expected were only the UV-pigment expressed and functional (Fig. 5 B), it follows that dim-flash responses obtained in response to such midwave stimuli represent transduction driven purely by the M-pigment, while responses to dim 361-nm flashes represent transduction driven at least 85% by the UV-pigment (85% is the "worst case," in which the two pigments are coexpressed in 1:1 ratio). It is thus possible to compare the kinetics of phototransduction activated in individual cells by one or the other cone pigment. To perform this comparison, a series of dim UV or midwave flashes were presented to a cell, with intensities selected to suppress no more than 35% of the current. Saturating flashes were interleaved with dim

flashes to monitor the circulating current level, and comparisons between UV-cone pigment–driven and M-cone pigment–driven responses deemed valid only when the traces met a strict criterion of reversibility, i.e., when the time course of the dim-flash responses to the ultraviolet flashes before and after the period of midwave stimulation were indiscriminable to inspection. Results from cells investigated with this protocol (Fig. 7 A) show little difference in the kinetics of responses driven by the UV-cone pigment (purple traces) as compared with the responses driven by the M-cone pigment (green traces). Nonetheless, there was a reliable tendency for the M-cone responses to recover more slowly, a tendency that led us to investigate further the hypothesis that the two pigments might have distinct inactivation mechanisms, as we now describe.

### *Differential Dependence of UV- and M-cone Pigment Inactivation on the G-protein Receptor Kinase, Grk1*

The functional coexpression of both UV- and M-cone pigments in *Nrl* $^{-/-}$ photoreceptors provides a special opportunity for the investigation of the dependence of cone pigment inactivation on G-protein–coupled receptor kinase. The only such kinase in the mouse genome known to be expressed in cones is Grk1, also known as "rhodopsin kinase" for its well-established role in the inactivation of rhodopsin in rods (Chen et al., 1999, 2001). We thus undertook recordings from the photoreceptors of *Nrl* $^{-/-}$ mice that had been crossbred with *Grk1* $^{-/-}$ mice (Chen et al., 1999) to create mice with the double-knockout genotype, *Nrl* $^{-/-}$/*Grk1* $^{-/-}$ (Zhu et al., 2003). Dim-flash responses from a sample of cells from double-knockout mice are show in Fig. 7 B; in every case, the dim-flash response driven by the M-cone pigment was severely retarded in its recovery relative to the response driven by the UV-cone pigment. Again, comparisons between responses driven by the two pigments were only deemed valid when the responses to ultraviolet flashes collected before and after the responses to the midwave flashes had indistinguishable kinetics. It is evident that in the absence of Grk1 the M-cone pigment–driven responses recover much more slowly than those driven by the UV-cone pigment.

To quantify the comparisons of the recovery kinetics of the responses driven by the two cone pigments in individual cells, we measured a simple feature of the dim-flash response, its full-width at half-maximum, or $\Delta T_{50}$ (Fig. 8 A). $\Delta T_{50}$s for the UV- and M-cone pigment–driven responses for animals of the two genotypes are summarized in the bar chart of Fig. 8 B. While the deletion of Grk1 slowed the recovery of responses driven by both pigments, the effect on the M-pigment response was much larger; thus, in the absence of Grk1, the average $\Delta T_{50}$ of the response to the M-pigment increased

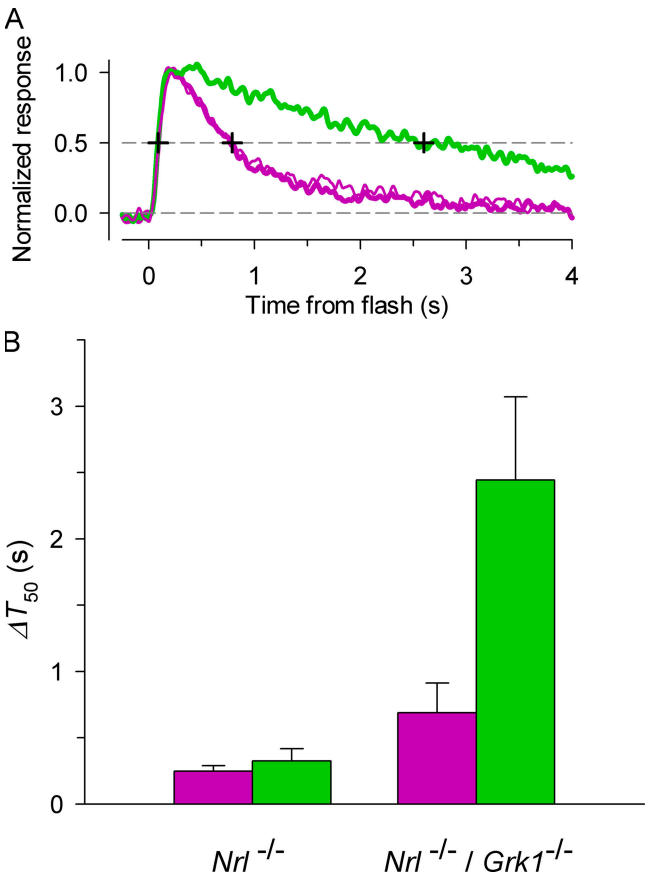


FIGURE 8. Quantitative comparison of the recoveries of dim-flash responses of photoreceptors of *Nrl* $^{-/-}$ mice or *Nrl* $^{-/-}$/*Grk1* $^{-/-}$ mice, driven by either the UV-cone pigment (purple) or M-cone pigment (green). (A) Method of quantification: the full width half-maximum ($\Delta T_{50}$) of the normalized dim-flash response was determined from the intersection of the traces with a line at 50% amplitude; three intersections are illustrated by cross-hairs superimposed on the traces. $\Delta T_{50}$ is the interval between the initial intersection with the response rising phase and the second intersection with the recovery phase. (B) Histograms of the $\Delta T_{50}$s for the UV-cone pigment (purple bars) and M-cone pigment–driven responses (green bars) from populations of cells from animals of the two genotypes (*Nrl* $^{-/-}$, $n = 17$ cells; *Nrl* $^{-/-}$/*Grk1* $^{-/-}$, $n = 9$ cells); the error bars are 95% confidence intervals. Statistical analysis showed that all the values of $\Delta T_{50}$ represented in Fig. 6 B are significantly different from one another on the basis of *t* tests (two samples, unequal variance, one-tail): for *Nrl* $^{-/-}$ cells, UV vs. M-opsin–driven responses, $P < 0.032$; for *Nrl* $^{-/-}$/*Grk1* $^{-/-}$ cells, UV vs. M-opsin–driven responses, $P < 10^{-4}$; for UV-opsin–driven responses of *Nrl* $^{-/-}$ cells vs. *Nrl* $^{-/-}$/*Grk1* $^{-/-}$ cells, $P < 10^{-3}$; for M-opsin–driven responses of *Nrl* $^{-/-}$ cells vs. *Nrl* $^{-/-}$/*Grk1* $^{-/-}$ cells, $P < 10^{-4}$. There was no statistically reliable difference between the $\Delta T_{50}$s of the "pre" and "post" UV-driven responses, and so the $\Delta T_{50}$s of these responses were averaged for the histogram analysis. In other words, the traces of all cells obeyed the reversibility criterion illustrated in Fig. 7 and in panel A of this figure.

7.5-fold (from 0.33 to 2.44 s), while the $\Delta T_{50}$ of the UV-pigment response increased 2.8-fold (from 0.25 to 0.69 s); both these differences in $\Delta T_{50}$ are highly significant ($P < 0.0004$), arguing strongly that Grk1 is necessary

for normal inactivation of both pigments. Since the recordings used for comparison of dim-flash responses were made with the outer segment drawn into the suction pipette, caution is called for in interpreting the absolute numerical values of the $\Delta T_{50}$s. Nonetheless, as comparisons were only made when the UV-pigment–driven response was unchanged throughout the recording epoch, it can be concluded that the inactivation of the M-cone pigment is more severely affected by the absence of Grk1 than that of the UV-cone pigment.

### *Comparison of the Kinetic Properties of Nrl $^{-/-}$ Photoreceptors and WT Rods*

It is of major importance to determine whether *Nrl* $^{-/-}$ photoreceptors are to be classified as cones or possibly as "a species of photoreceptor intermediate between cones and rods" (Mears et al., 2001). While a definitive classification requires comparison of these cells with WT rods and cones on a battery of ultrastructural, histochemical, molecular, and physiological features (Daniele et al., 2005), it is nonetheless useful for the classification effort to compare the features of the photoresponses of individual *Nrl* $^{-/-}$ photoreceptors with those of WT rods recorded under the same conditions. Our investigation shows that in addition to their distinguishing spectral sensitivities, individual *Nrl* $^{-/-}$ photoreceptors have response properties that are highly distinctive from those of rods. Here we summarize those distinctive properties, giving the results from populations of cells recorded in either the OS-in or OS-out configuration (Fig. 9; Table I). In addition to dividing the data according to the recording configuration, we have further subdivided the data of *Nrl* $^{-/-}$ photoreceptors recorded in the OS-in configuration into three subgroups, based on the time to peak of the dim-flash response. This subdivision is to some degree arbitrary, but serves to assist in comparative assessment of the features of *Nrl* $^{-/-}$ photoreceptors recorded in this configuration with those of WT rods.

*Time to peak ($t_{peak}$).* In the OS-out configuration, the time to peak of the dim-flash response of *Nrl* $^{-/-}$ photoreceptors was $t_{peak}$ = 91 ± 6 ms (mean ± 95% c.i.), more than twofold shorter than that of rods in the configuration that gave the shorter value, $t_{peak}$ = 200 ± 20 ms (Fig. 9 A; $P < 10^{-7}$, one-tailed *t* test).

*Dominant Time Constant of Recovery ($\tau_D$).* The dominant recovery time constant for just-saturating flashes (cf. Fig. 3) was reliably shorter in *Nrl* $^{-/-}$ photoreceptors recorded in the OS-out configuration as compared with rods in the configuration that gave the shorter value: $\tau_D$ = 110 ± 40 ms vs. $\tau_D$ = 210 ± 40 ms (Fig. 9 B; $P < 0.0004$, one-tailed *t* test).

*Half-saturating Flash Intensity ($Q_{1/2}$).* The flash intensities that produced half-saturating responses of *Nrl* $^{-/-}$ photoreceptors were close to 100-fold higher than those that half saturated rod responses. Our rod results ($Q_{1/2}$ = 40 ± 10 photons μm$^{-2}$, mean ± s.d.) are in good agreement with previous reports: $Q_{1/2}$ = 30 ± 6 photons μm$^{-2}$ (Howes et al., 2002); 49 ± 3 (Xu et al., 1997), 55 ± 5 (Calvert et al., 2000), 60 ± 10 (Calvert et al., 2001), and 67 ± 6 (Chen et al., 1999).

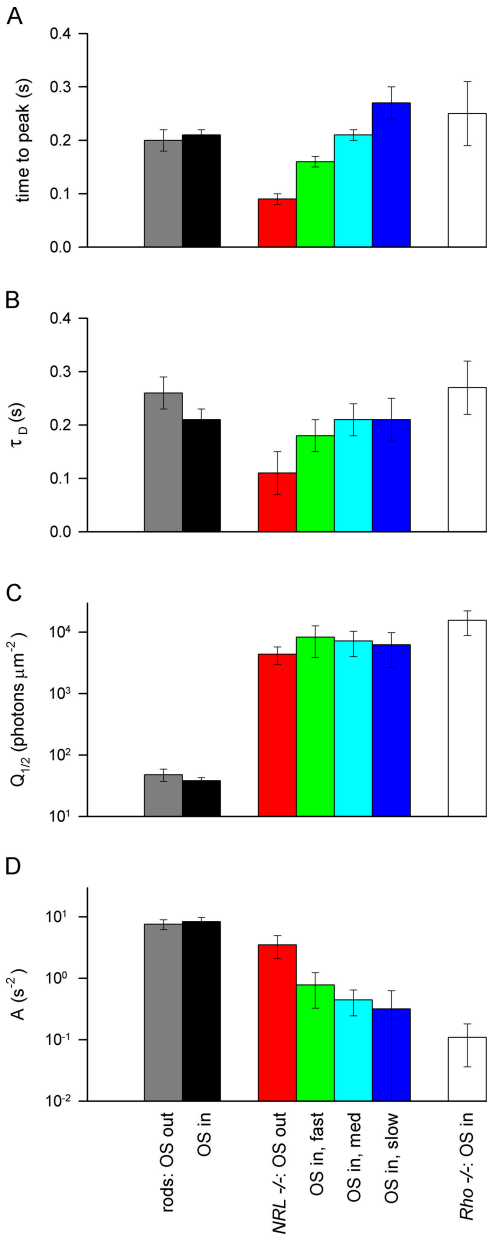


FIGURE 9. Comparison of response properties of WT rods, *Nrl* $^{-/-}$ and *Rho* $^{-/-}$ photoreceptors. Responses of WT rods were recorded with the outer segment either in the suction electrode (OS in, black bars, $n$ = 10) or with a portion of the inner segment drawn into the pipette (OS out, gray bars, $n$ = 13). Similarly, *Nrl* $^{-/-}$ photoreceptors were recorded in both configurations (OS out, red bars, $n$ = 8; OS in, green, $n$ = 12; cyan, $n$ = 13; and blue, $n$ = 5), with the latter groups subdivided based on the time-to-peak of the dim-flash response (A). *Rho* $^{-/-}$ cells were recorded only the OS-in configuration (clear bars, $n$ = 8).

*Flash Sensitivity, Expressed as Fraction of Circulating Current Suppressed per Photoisomerization.* For interpretation in terms of the intrinsic properties of phototransduction, flash sensitivity is best expressed in terms of fraction circulating current suppressed per photoisomerization. To do this, flash intensities expressed in photons $\mu m^{-2}$ are multiplied by the collecting area, $a_C$ expressed in $\mu m^2$ (MATERIALS AND METHODS). At the peak of the dim-flash response, 5.4 ± 1.3% of the rod circulating current was suppressed per photoisomerization; in contrast, only ~0.24% of the circulating current of the *Nrl* $^{-/-}$ photoreceptors was suppressed per photoisomerization (Table I), a 40-fold lower sensitivity than rods. Comparable differences in rod and cone sensitivities expressed in photoisomerizations have been reported for other mammalian species, e.g., 5 ± 1.5% for primate rods (Baylor et al., 1984) vs. 0.2% for primate cones (Schnapf et al., 1990).

*Amplification Coefficient (A).* The amplification coefficient of *Nrl* $^{-/-}$ photoreceptors in the OS-out configuration was 2.2-fold lower than that of rods: $A = 3.5 \pm 1.4$ $s^{-2}$ vs. $A = 8.0 \pm 1.0$ $s^{-2}$. As mentioned above, *Nrl* $^{-/-}$ photoreceptors recorded in the OS-in configuration had considerably reduced amplification (Fig. 3 B; Fig. 9 D).

### *Recordings from Rho$^{-/-}$ Cones*

Despite a great effort, we were only able to make a small number of recordings from the cones of rhodopsin knockout (*Rho*$^{-/-}$) mice, which like *Nrl* $^{-/-}$ mice have no rod outer segments (Table I; Fig. 9). Remarkably, slices of these retinas appear to have a large number of cone outer segments, but very few generate a measurable photocurrent, and those that did decayed even more rapidly in their function than *Nrl* $^{-/-}$ photoreceptors recorded in the OS-in configuration. At present, no strong conclusions can be drawn, but it is notable that *Rho*$^{-/-}$ outer segments appeared to be even more fragile and labile that those of *Nrl* $^{-/-}$ photoreceptors.

### *Final Perspectives*

To provide a final perspective on the comparison of the kinetics of WT rods and *Nrl* $^{-/-}$ photoreceptors, we have plotted the average dim-flash responses of the two cell types (Fig. 10). *Nrl* $^{-/-}$ photoreceptors in the OS-out configuration (red trace in Fig. 10, A and B) are faster in their recovery kinetics than in the OS-in configuration (green trace in Fig. 10 B), whereas the dim-flash responses of rods were very similar in the two recording configurations (Fig. 10 B). Clearly, *Nrl* $^{-/-}$ photoreceptors in the OS-out configuration have much faster response recoveries than do rods, but a subpopulation of *Nrl* $^{-/-}$ photoreceptors recorded in the OS-in configuration also had reliably faster recoveries (green traces, Fig. 10 B).

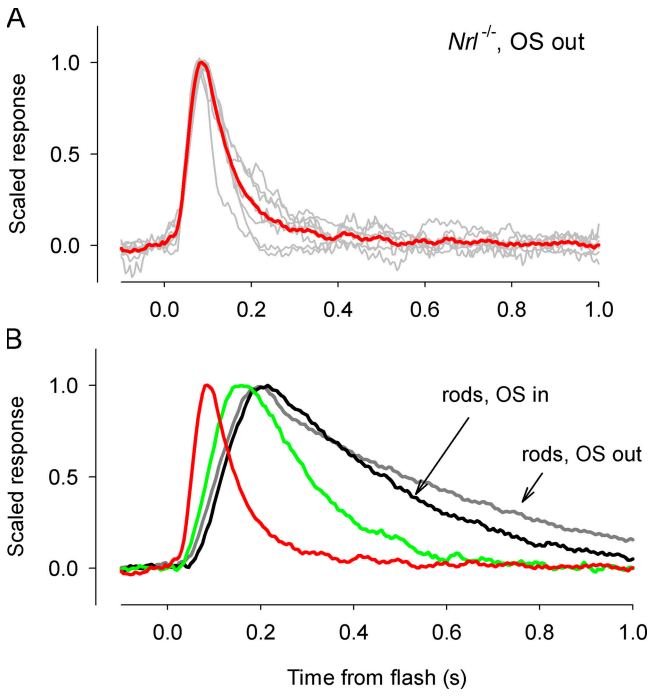


FIGURE 10. Comparison of the normalized dim-flash responses of *Nrl* $^{-/-}$ photoreceptors and WT rods. (A) Responses of the population of *Nrl* $^{-/-}$ photoreceptors whose responses were recorded in the OS-out configuration are all shown (gray traces), along with their average (red trace). (B) Dim-flash responses of rods recorded in the two configurations are compared with those of *Nrl* $^{-/-}$ photoreceptors; the green trace presents the average response of the subpopulation of *Nrl* $^{-/-}$ photoreceptors recorded in the OS-in configuration whose data are summarized in the histogram of Fig. 9 with green bars; the red trace is the same as that illustrated in A.

## DISCUSSION

### *Nrl $^{-/-}$ Photoreceptors Are Properly Classified as Cones*

The single-cell electrophysiological results reported here, combined with electron microscopy (EM), immunohistochemistry, protein analysis, and electroretinographic (*a*-wave) analysis, lead to the conclusion that *Nrl* $^{-/-}$ photoreceptors are a species of cones. At the EM level, the number of open basal discs and the size and shape of mitochondria clearly identify *Nrl* $^{-/-}$ photoreceptors as cones (Carter-Dawson and LaVail, 1979; unpublished data). At the histochemical level, each *Nrl* $^{-/-}$ photoreceptor has associated with it an extracellular matrix sheath that is stained by the plant lectin, peanut agglutinin or PNA (Daniele et al., 2005), a unique characteristic of cones, including the cones of WT mice (Blanks and Johnson, 1983; Johnson et al., 1986; Blanks et al., 1988). Like WT cones, *Nrl* $^{-/-}$ photoreceptors express both UV- and M-cone opsins, and when photoactivated, both cone pigments drive phototransduction in the absence of rod transducin, rod phosphodiesterase, and rod cGMP channels (Mears et al.,

2001), while cone isoforms of these proteins are expressed in abundance (Mears et al., 2001; Daniele et al., 2005). When measured either in situ with paired-flash a-wave methods (Daniele et al., 2005), or measured with suction pipette recordings in the OS-out configuration, the dim-flash responses and recovery kinetics of *Nrl* $^{-/-}$ photoreceptors are highly reliably faster than those of WT rods (Table I; Figs. 3, 9, and 10). The average time to peak of the dim-flash responses ($t_{peak}$ = 91 ms) is, however, somewhat slower than those previously reported for other mammalian S-cones: macaque, $t_{peak}$ = 60 ms (Schnapf et al., 1990); ground squirrel $t_{peak}$ = 30 ± 9 ms, (Kraft, 1988).

### *Functional Coexpression of UV- and M-cone Pigments in Nrl $^{-/-}$ and Rho $^{-/-}$ Photoreceptors*

The results presented here establish incontrovertibly for the first time that the photoreceptors of *Nrl* $^{-/-}$ and *Rho* $^{-/-}$ mice functionally coexpress both the UV- and M-cone pigments (Fig. 5); that is, both cone pigments drive phototransduction in the individual cells, consistent with expectations from WT mice and other rodents based on immunohistochemistry (Rohlich et al., 1994; Applebury et al., 2000; Dkhissi-Benyahya et al., 2001; Lukats et al., 2002). The results further establish that the coexpression ratio of M- to UV-pigments varies ~1000-fold, reflecting a positional gradient in the retina (Fig. 2; Fig. 5 B), well documented in WT mouse cones (Applebury et al., 2000; Fei and Hughes, 2001). Functional coexpression of a UV-pigment and one or more midwave to longwave pigments has been previously shown in recordings of single salamander cones (Makino and Dodd, 1996), but the work presented here provides the first demonstration of functional coexpression in mammalian cones.

The dim-flash responses driven by the two pigments in *Nrl* $^{-/-}$ photoreceptors differ little in kinetics (Fig. 7 A), implying that phototransduction activated by the two pigments is quite similar. Nonetheless, responses driven by the M-pigment recover reliably if only slightly more slowly than responses driven by the UV-pigment in some cells (Fig. 7 A; Fig. 8). Genomic information on the mouse indicates that (as in other mammals) there is only one cone transducin (Gnat2), and certainly the remaining proteins of the transduction cascade are the same regardless of which pigment is activated in a cell. Hence, the most likely explanation of this slight difference in recovery kinetics is that the UV- and M-pigments are inactivated differently.

### *Functional Coexpression of S- and M-cone Pigments in Rodent Photoreceptors and Color Vision*

A basic insight of color science is that "color vision," operationally defined as the ability to discriminate of stimuli on the basis of their spectral content, requires at least two visual pigments and, further, requires that the signals generated by the photoreceptors containing the two pigments be encoded neurally in a manner that preserves their distinct information. The functional coexpression of S- and M-cone pigments in rodent photoreceptors appears to be at odds with this basic requirement for color vision proper and seems to pose a problem as to why rodent cones would express two pigments. The solution to this conundrum is that the view that "cones are for color vision" is misguided. The most important function of cones in vision is to provide useful visual signals in daylight, even under conditions when most of their visual pigment is bleached. Indeed, the steady-state response of cones never saturates in steady illumination, no matter how intense (Burkhardt, 1994). Beyond the prime directive of cones to give signals in bright light there is additional survival value to sampling different portions of the spectrum. Such spectral sampling by two pigments needn't be encoded in separate neural channels to be useful to the organism. Functional coexpression of S- and M-opsin, with the latter expressed in a dorso-ventral gradient (Fig. 1) no doubt samples the spectrum of the sky and the ground in a manner that provides information of survival value to rodents. Moreover, it seems possible that despite cone pigment coexpression, mice could learn to discriminate spectrally pure stimuli (e.g., 400 vs. 500 nm) independent of relative intensity (and thus appear to have a rudimentary form of color vision) based on the unique dorso-ventral pattern that each stimulus would produce. Thus, independent of its absolute intensity, a 400-nm stimulus of large angular extent would produce a higher level of excitation in the ventral than in the dorsal retina, while a 500-nm stimulus would produce the opposite. The encoding of the differing dorso-ventral gradients resulting of the two stimuli could be done with a single neural channel, in effect generating a distinct retinotopic pattern of neural excitation for stimuli of different wavelengths, even though the physical stimuli are spatially homogeneous. Discrimination based on such retinotopic gradients would not qualify as color vision proper, which requires that such stimuli be discriminable when the retina is stimulated locally. However, such a mechanism could conceivably underlie the discriminability found in a recent behavioral investigation by Jacobs et al. (2004).

### *Both the UV-cone Pigment and S-cone Pigment Require Grk1 for Normal Inactivation*

Genomic analysis and histochemistry (Chen et al., 2001; Weiss et al., 2001; Caenepeel et al., 2004) indicate that only one GPCR kinase known to phosphorylate opsins, Grk1 (alias "rhodopsin kinase"), is expressed in mouse photoreceptors. In particular GRK7, an apparently more ancient kinase that is strongly expressed in

the cones of many species, is completely absent in mouse (Chen et al., 2001; Weiss et al., 2001; Tachibanaki et al., 2001), although evolutionary analysis of genomic information suggests that it was present in the common ancestor of primates and mice (Caenepeel et al., 2004). Recent work has shown that the light-exposed UV-pigment is phosphorylated in the *Nrl*$^{-/-}$ retina, but not in retinas of *Nrl*$^{-/-}$*/Grk1*$^{-/-}$ (Zhu et al., 2003), providing indirect evidence that Grk1 is involved in mouse S-pigment inactivation. Our recordings from *Nrl*$^{-/-}$*/Grk1*$^{-/-}$ photoreceptors (Fig. 7 B; Fig. 8) show that the recovery phase of dim-flash responses driven by either the UV- or M-cone pigment is slowed by the deletion of Grk1, establishing definitively that Grk1 is necessary for the normal inactivation of the mouse cone photoresponse, as previously inferred from cone-driven electroretinographic responses of *Grk1*$^{-/-}$ mice (Lyubarsky et al., 2000).

### *The Inactivation of the M-cone Pigment Is More Severely Slowed by Grk1 Deletion*

The possibility of recording dim-flash responses from individual photoreceptors driven by either the UV- or the M-cone pigment produced a major surprise: the M-cone pigment–driven responses recover much more slowly than the UV-cone pigment–driven responses in the absence of Grk1 (Figs. 7 and 8). This result implies that there are important differences between the two cone pigments in their requirement for Grk1 for inactivation and, in particular, leads to the hypothesis that the UV-cone pigment has a Grk1-independent mechanism of inactivation that is faster than that of the M-cone pigment. One example of such an hypothesis is that the spontaneous hydrolysis of the all-trans chromophore from its Schiff-base attachment in the Metarhodopsin II/Metarhodopsin III states is faster in the UV- pigment than in the M-pigment (Vought et al., 1999). Another example would be the presence of an as yet undetected Grk or other kinase, although such a kinase would have to have a strong preference for S-opsin over M-opsin as a substrate. In this context, it bears mention that in fish, Grk7 appears to be more efficient in inactivating rhodopsin than Grk1 (Tachibanaki et al., 2001); given that S-opsins have greater homology with rhodopsin than with M-cone opsins, if another kinase is responsible for the relatively faster inactivation of S-opsin in the absence of Grk1, it would have an unusual substrate specificity.

### *The Rate of Activation of Phosphodiesterase per Photoisomerization in Nrl*$^{-/-}$ *Photoreceptors Is Reduced Relative to that in WT Rods*

The amplification constant, extracted from analysis of the activation phase of the response of photoreceptors, quantifies the accelerating closure of cGMP channels as the photoactivated pigment (R*) activates its transducin, transducins activate phosphodiesterase (PDE), and cGMP declines (Lamb and Pugh, 1992; Pugh and Lamb, 1993; Leskov et al., 2000). The average amplification constant of WT rods ($A$ = 8.0 s$^{-2}$) is 2.3-fold higher than that of *Nrl*$^{-/-}$ photoreceptors ($A$ = 3.5 s$^{-2}$; OS-out configuration) (Table I). Theory predicts $A$ to be inversely proportional to the OS cytoplasmic volume, $V_{cyto}$ (Lamb and Pugh, 1992), and analysis of rods having different OS volumes has confirmed this prediction (Pugh and Lamb, 1993). Given that the Hill coefficient of the cGMP-activated channels in both types of photoreceptors is the same (Yau, 1994), and that the kinetic parameters ($k_{cat}$ and $K_m$) of the cone PDE are comparable to those of the rod PDE (Gillespie and Beavo, 1988; Gillespie, 1990), it follows from the inverse dependence of $A$ on $V_{cyto}$ and the volume ratio of the WT rod OS to the *Nrl*$^{-/-}$ OS, 4.5, that the rate of activation of PDEs per R* is ~10-fold lower in *Nrl*$^{-/-}$ cells than in rods.

The amplification coefficients of both rods and *Nrl*$^{-/-}$ photoreceptors estimated from the single-cell recordings presented here are close to estimates obtained from ERG a-wave data; for rods, $A$ = 8.0 s$^{-2}$ (single cells, Table I) vs. 7.4 s$^{-2}$ (WT ERG a-waves, 8 wk olds; Lyubarsky et al., 2004); $A$ = 3.5 s$^{-2}$ (single *Nrl*$^{-/-}$ cells, OS out, Table I), vs. 4.0 s$^{-2}$ (ERG a-waves, 4–6-wk-old *Nrl*$^{-/-}$ mice; Daniele et al., 2005). It bears mention that the end-on collecting area of *Nrl*$^{-/-}$ photoreceptors in vivo, required to estimate amplification from a-wave data, was hypothesized to be increased fourfold by light funneling in the inner segment. This hypothesis is supported by the dimensions of the *Nrl*$^{-/-}$ photoreceptor inner segment, which electron microscopy reveals to taper steeply to the outer segment (Daniele et al., 2005).

### *The Decreased Amplification and Speed of Nrl*$^{-/-}$ *Photoreceptors in the OS-in Configuration Suggests that Mouse Cones Removed from their Matrix Sheath Deteriorate*

The changes in the properties of the responses of *Nrl*$^{-/-}$ photoreceptors recorded with the OS drawn into the suction electrode (Fig. 4) suggest that these outer segments are more labile than those of WT rods. One explanation is that the suction pipette itself may damage the outer segment in the OS-in configuration. An alternative, and not mutually exclusive, hypothesis is that damage may begin before drawing the cell into the suction pipette. Like WT mouse cones, each *Nrl*$^{-/-}$ photoreceptor has a PNA-stained extracellular matrix, which appears to be attached to the inner segment and which ensheaths the outer segment (Daniele et al., 2005). Since the cone matrix sheath makes adhesions with both the cone and the RPE apical surface, the removal of the retina from the RPE necessarily disrupts the at-

tachment of the cone sheath to the RPE, and likely also disrupts attachment of the sheath to cones (Johnson et al., 1986; Hageman et al., 1995). Damage to or loss of these attachments could compromise the cone disc membranes.

### *The Nrl $^{-/-}$ Retina as a Preparation for the Investigation of Mammalian Cone Function*

Because of the power of mouse genetics and molecular biology, the *Nrl* $^{-/-}$ retina holds much promise as a preparation for the investigation of cone physiological and biochemical function, and for the identification of molecules involved in cone-specific genetic disease. The recent characterization of the dependence of mouse UV-cone pigment phosphorylation and cone arrestin binding on Grk1 (Zhu et al., 2003) constitutes an initial realization of the first promise, and the genetic characterization of a large set of genes whose expression is enriched in the *Nrl* $^{-/-}$ retina (Yoshida et al., 2004) provides a foundation for the second. The degree to which the gene expression profiles and physiological response properties of *Nrl* $^{-/-}$ photoreceptors correspond to those of WT mouse cones will ultimately be resolved by physiological experiments and gene expression analyses. Meanwhile, the conclusion that *Nrl* $^{-/-}$ photoreceptors are indeed a species of cones opens the door to many investigations of fundamental importance to the understanding of molecular function in cones, and ways in which mutations of genes expressed specifically in cones and nearby cells leads to their demise.

We thank Dr. J. Lem (Tufts University School of Medicine, Boston, MA) for providing rhodopsin$^{-/-}$ mice, and Dr. C.-K. Chen (University of Utah Health Sciences Center, Salt Lake City, UT) for providing *Grk1*$^{-/-}$ mice.

E.N. Pugh Jr. is supported by a Jules and Doris Stein Research to Prevent Blindness Professorship, and C.M. Craft is supported by the Mary D. Allen Chair in Vision Research of the Doheny Eye Research Institute. This work was also supported by NIH-EY-02660; EY-11115; EY-00395, The Foundation Fighting Blindness; and Research to Prevent Blindness Foundation.

Lawrence G. Palmer served as editor.

*Submitted: 4 November 2004*
*Accepted: 2 February 2005*

REFERENCES

Ahnelt, P.K. 1998. The photoreceptor mosaic. *Eye.* 12:531–540.

Applebury, M.L., M.P. Antoch, L.C. Baxter, L.L. Chun, J.D. Falk, F. Farhangfar, K. Kage, M.G. Krzystolik, L.A. Lyass, and J.T. Robbins. 2000. The murine cone photoreceptor: a single cone type expresses both S and M opsins with retinal spatial patterning. *Neuron.* 27:513–523.

Baylor, D.A., T.D. Lamb, and K.-W. Yau. 1979a. Responses of retinal rods to single photons. *J. Physiol.* 288:613–634.

Baylor, D.A., T.D. Lamb, and K.-W. Yau. 1979b. The membrane current of single rod outer segments. *J. Physiol.* 288:589–611.

Baylor, D.A., B.J. Nunn, and J.L. Schnapf. 1984. The photocurrent, noise and spectral sensitivity of rods of the monkey *Macaca fascicularis*. *J. Physiol.* 357:575–607.

Blanks, J.C., G.S. Hageman, L.V. Johnson, and C. Spee. 1988. Ultrastructural visualization of primate cone photoreceptor matrix sheaths. *J. Comp. Neurol.* 270:288–300.

Blanks, J.C., and L.V. Johnson. 1983. Selective lectin binding of the developing mouse retina. *J. Comp. Neurol.* 221:31–41.

Burkhardt, D.A. 1994. Light adaptation and photopigment bleaching in cone photoreceptors in situ in the retina of the turtle. *J. Neurosci.* 14:1091–1105.

Burns, M.E., A. Mendez, J. Chen, and D.A. Baylor. 2002. Dynamics of cyclic GMP synthesis in retinal rods. *Neuron.* 36:81–91.

Caenepeel, S., G. Charydczak, S. Sudarsanam, T. Hunter, and G. Manning. 2004. The mouse kinome: discovery and comparative genomics of all mouse protein kinases. *Proc. Natl. Acad. Sci. USA.* 101:11707–11712.

Calvert, P.D., V.I. Govardovskii, N. Krasnoperova, R.E. Anderson, J. Lem, and C.L. Makino. 2001. Membrane protein diffusion sets the speed of rod phototransduction. *Nature.* 411:90–94.

Calvert, P.D., N.V. Krasnoperova, A.L. Lyubarsky, T. Isayama, M. Nicolo, B. Kosaras, G. Wong, K.S. Gannon, R.F. Margolskee, R.L. Sidman, et al. 2000. Phototransduction in transgenic mice after targeted deletion of the rod transducin alpha-subunit. *Proc. Natl. Acad. Sci. USA.* 97:13913–13918.

Carter-Dawson, L.D., and M.M. LaVail. 1979. Rods and cones in the mouse retina. I. Structural analysis using light and electron microscopy. *J. Comp. Neurol.* 188:245–262.

Chen, C.K., M.E. Burns, W. He, T.G. Wensel, D.A. Baylor, and M.I. Simon. 2000. Slowed recovery of rod photoresponse in mice lacking the GTPase accelerating protein RGS9-1. *Nature.* 403:557–560.

Chen, C.K., M.E. Burns, M. Spencer, G.A. Niemi, J. Chen, J.B. Hurley, D.A. Baylor, and M.I. Simon. 1999. Abnormal photoresponses and light-induced apoptosis in rods lacking rhodopsin kinase. *Proc. Natl. Acad. Sci. USA.* 96:3718–3722.

Chen, C.K., K. Zhang, J. Church-Kopish, W. Huang, H. Zhang, Y.J. Chen, J.M. Frederick, and W. Baehr. 2001. Characterization of human GRK7 as a potential cone opsin kinase. *Mol. Vis.* 7:305–313.

Chen, J., C.L. Makino, N.S. Peachey, D.A. Baylor, and M.I. Simon. 1995. Mechanisms of rhodopsin inactivation in vivo as revealed by a COOH-terminal truncation mutant. *Science.* 267(5196):374–377.

Cobbs, W.H., and E.N. Pugh Jr. 1987. Kinetics and components of the flash photocurrent of isolated retinal rods of the larval salamander, *Ambystoma tigrinum*. *J. Physiol.* 394:529–572.

Cornish, E.E., M. Xiao, Z. Yang, J.M. Provis, and A.E. Hendrickson. 2004. The role of opsin expression and apoptosis in determination of cone types in human retina. *Exp. Eye Res.* 78:1143–1154.

Daniele, L.L., C. Lillo, A.L. Lyubarsky, S.S. Nikonov., N. Philp, A.J. Mears, A. Swaroop, D.S. Williams, and E.N. Pugh Jr. 2005. Cone-like morphological, molecular and electrophysiological features of the photoreceptors of the *Nrl* knockout mouse. *Investigative Ophthalmology and Visual Science.* In press.

Dkhissi-Benyahya, O., A. Szel, W.J. Degrip, and H.M. Cooper. 2001. Short and mid-wavelength cone distribution in a nocturnal Strepsirrhine primate (*Microcebus murinus*). *J. Comp. Neurol.* 438:490–504.

Ebrey, T., and Y. Koutalos. 2001. Vertebrate photoreceptors. *Prog. Retin. Eye Res.* 20:49–94.

Fei, Y., and T.E. Hughes. 2001. Transgenic expression of the jellyfish green fluorescent protein in the cone photoreceptors of the mouse. *Vis. Neurosci.* 18:615–623.

Gillespie, P.G. 1990. Phosphodiesterases in visual transduction by rods and cones. *In* Cyclic Nucleotide Phosphodiesterases: Struc-

ture, Regulation and Drug Action. J. Beavo and M.D. Houslay, editors. Wiley, New York. 163–184.

Gillespie, P.G., and J.A. Beavo. 1988. Characterization of a bovine cone photoreceptor phosphodiesterase purified by cyclic GMP-sepharose chromatography. *J. Biol. Chem.* 263:8133–8141.

Govardovskii, V.I., N. Fyhrquist, T. Reuter, D.G. Kuzmin, and K. Donner. 2000. In search of the visual pigment template. *Vis. Neurosci.* 17:509–528.

Hageman, G.S., M.F. Marmor, X.Y. Yao, and L.V. Johnson. 1995. The interphotoreceptor matrix mediates primate retinal adhesion. *Arch. Ophthalmol.* 113:655–660.

Hagins, W.A., R.D. Penn, and S. Yoshikami. 1970. Dark current and photocurrent in retinal rods. *Biophys. J.* 10:380–412.

Harosi, F.I. 1982. Polarized microspectrophotometry for pigment orientation and concentration. *Methods Enzymol.* 81:642–647.

Hendrickson, A., and D. Hicks. 2002. Distribution and density of medium- and short-wavelength selective cones in the domestic pig retina. *Exp. Eye Res.* 74:435–444.

Howes, K.A., M.E. Pennesi, I. Sokal, J. Church-Kopish, B. Schmidt, D. Margolis, J.M. Frederick, F. Rieke, K. Palczewski, S.M. Wu, et al. 2002. GCAP1 rescues rod photoreceptor response in GCAP1/GCAP2 knockout mice. *EMBO J.* 21:1545–1554.

Jacobs, G.H., G.A. Williams, and J.A. Fenwick. 2004. Influence of cone pigment coexpression on spectral sensitivity and color vision in the mouse. *Vision Res.* 44:1615–1622.

Johnson, L.V., G.S. Hageman, and J.C. Blanks. 1986. Interphotoreceptor matrix domains ensheath vertebrate cone photoreceptor cells. *Invest. Ophthalmol. Vis. Sci.* 27:129–135.

Kraft, T.W. 1988. Photocurrents of cone photoreceptors of the golden-mantled ground squirrel. *J. Physiol.* 404:199–213.

Lamb, T.D. 1995. Photoreceptor spectral sensitivities: common shape in the long-wavelength region. *Vision Res.* 35:3083–3091.

Lamb, T.D., and E.N. Pugh Jr. 1992. A quantitative account of the activation steps involved in phototransduction in amphibian photoreceptors. *J. Physiol.* 449:719–758.

Lem, J., N.V. Krasnoperova, P.D. Calvert, B. Kosaras, D.A. Cameron, M. Nicolo, C.L. Makino, and R.L. Sidman. 1999. Morphological, physiological, and biochemical changes in rhodopsin knockout mice. *Proc. Natl. Acad. Sci. USA.* 96:736–741.

Leskov, I.B., V.A. Klenchin, J.W. Handy, G.G. Whitlock, V.I. Govardovskii, M.D. Bownds, T.D. Lamb, E.N. Pugh Jr., and V.Y. Arshavsky. 2000. The gain of rod phototransduction: reconciliation of biochemical and electrophysiological measurements. *Neuron.* 27:525–537.

Liebman, P.A. 1972. Microspectrophotometry of photoreceptors. *In* Handbook of Sensory Physiology. H.J.A. Dartnall, editor. Springer, New York. 481–528.

Lukats, A., O. Dkhissi-Benyahya, Z. Szepessy, P. Rohlich, B. Vigh, N.C. Bennett, H.M. Cooper, and A. Szel. 2002. Visual pigment coexpression in all cones of two rodents, the Siberian hamster, and the pouched mouse. *Invest. Ophthalmol. Vis. Sci.* 43:2468–2473.

Lyubarsky, A.L., C. Chen, M.I. Simon, and E.N. Pugh Jr. 2000. Mice lacking G-protein receptor kinase 1 have profoundly slowed recovery of cone-driven retinal responses. *J. Neurosci.* 20:2209–2217.

Lyubarsky, A.L., B. Falsini, M.E. Pennesi, P. Valentini, and E.N. Pugh Jr. 1999. UV- and midwave-sensitive cone-driven retinal responses of the mouse: a possible phenotype for coexpression of cone photopigments. *J. Neurosci.* 19:442–455.

Lyubarsky, A.L., F. Naarendorp, X. Zhang, T. Wensel, M.I. Simon, and E.N. Pugh Jr. 2001. RGS9-1 is required for normal inactivation of mouse cone phototransduction. *Mol. Vis.* 7:71–78.

Lyubarsky, A.L., L.L. Daniele, and E.N. Pugh. 2004. From candelas to photoisomerizations in the mouse eye by rhodopsin bleaching in situ and the light-rearing dependence of the major components of the mouse ERG. *Vision Research.* 44:3235–3251.

Makino, C.L., and R.L. Dodd. 1996. Multiple visual pigments in a photoreceptor of the salamander retina. *J. Gen. Physiol.* 108:27–34.

Mears, A.J., M. Kondo, P.K. Swain, Y. Takada, R.A. Bush, T.L. Saunders, P.A. Sieving, and A. Swaroop. 2001. Nrl is required for rod photoreceptor development. *Nat. Genet.* 29:447–452.

Mendez, A., M.E. Burns, A. Roca, J. Lem, L.W. Wu, M.I. Simon, D.A. Baylor, and J. Chen. 2000. Rapid and reproducible deactivation of rhodopsin requires multiple phosphorylation sites. *Neuron.* 28:153–164.

Mendez, A., M.E. Burns, I. Sokal, A.M. Dizhoor, W. Baehr, K. Palczewski, D.A. Baylor, and J. Chen. 2001. Role of guanylate cyclase-activating proteins (GCAPs) in setting the flash sensitivity of rod photoreceptors. *Proc. Natl. Acad. Sci. USA.* 98:9948–9953.

Nikonov, S., N. Engheta, and E.N. Pugh Jr. 1998. Kinetics of recovery of the dark-adapted salamander rod photoresponse. *J. Gen. Physiol.* 111:7–37.

Okano, T., Y. Fukada, Y. Shichida, and T. Yoshizawa. 1992. Photosensitivities of iodopsin and rhodopsins. *Photochem. Photobiol.* 56: 995–1001.

Paupoo, A.A., O.A. Mahroo, C. Friedburg, and T.D. Lamb. 2000. Human cone photoreceptor responses measured by the electroretinogram a-wave during and after exposure to intense illumination. *J. Physiol.* 529:469–482.

Pennesi, M.E., K.A. Howes, W. Baehr, and S.M. Wu. 2003. Guanylate cyclase-activating protein (GCAP) 1 rescues cone recovery kinetics in GCAP1/GCAP2 knockout mice. *Proc. Natl. Acad. Sci. USA.* 100:6783–6788.

Pepperberg, D.R., J. Jin, and G.J. Jones. 1994. Modulation of transduction gain in light adaptation of retinal rods. *Vis. Neurosci.* 11: 53–62.

Pierce, E.A. 2001. Pathways to photoreceptor cell death in inherited retinal degenerations. *Bioessays.* 23:605–618.

Pugh, E.N., Jr., and T.D. Lamb. 1993. Amplification and kinetics of the activation steps in phototransduction. *Biochim. Biophys. Acta.* 1141:111–149.

Pugh, E.N., Jr., S. Nikonov, and T.D. Lamb. 1999. Molecular mechanisms of vertebrate photoreceptor light adaptation. *Curr. Opin. Neurobiol.* 9:410–418.

Rohlich, P., T. van Veen, and A. Szel. 1994. Two different visual pigments in one retinal cone cell. *Neuron.* 13:1159–1166.

Saari, J.C., M. Nawrot, B.N. Kennedy, G.G. Garwin, J.B. Hurley, J. Huang, D.E. Possin, and J.W. Crabb. 2001. Visual cycle impairment in cellular retinaldehyde binding protein (CRALBP) knockout mice results in delayed dark adaptation. *Neuron.* 29: 739–748.

Schnapf, J.L., B.J. Nunn, M. Meister, and D.A. Baylor. 1990. Visual transduction in cones of the monkey *Macaca fascicularis. J. Physiol.* 427:681–713.

Smith, N.P., and T.D. Lamb. 1997. The a-wave of the human electroretinogram recorded with a minimally invasive technique. *Vision Res.* 37:2943–2952.

Stone, E.M., T.A. Braun, S.R. Russell, M.H. Kuehn, A.J. Lotery, P.A. Moore, C.G. Eastman, T.L. Casavant, and V.C. Sheffield. 2004. Missense variations in the fibulin 5 gene and age-related macular degeneration. *N. Engl. J. Med.* 351:346–353.

Sun, H., J.P. Macke, and J. Nathans. 1997. Mechanisms of spectral tuning in the mouse green cone pigment. *Proc. Natl. Acad. Sci. USA.* 94:8860–8865.

Tachibanaki, S., S. Tsushima, and S. Kawamura. 2001. Low amplification and fast visual pigment phosphorylation as mechanisms characterizing cone photoresponses. *Proc. Natl. Acad. Sci. USA.* 98:14044–14049.

Vought, B.W., A. Dukkipatti, M. Max, B.E. Knox, and R.R. Birge.

1999. Photochemistry of the primary event in short-wavelength visual opsins at low temperature. *Biochemistry*. 38:11287–11297.

Weiss, E.R., M.H. Ducceschi, T.J. Horner, A. Li, C.M. Craft, and S. Osawa. 2001. Species-specific differences in expression of G-protein-coupled receptor kinase (GRK) 7 and GRK1 in mammalian cone photoreceptor cells: implications for cone cell phototransduction. *J. Neurosci*. 21:9175–9184.

Xiao, M., and A. Hendrickson. 2000. Spatial and temporal expression of short, long/medium, or both opsins in human fetal cones. *J. Comp. Neurol*. 425(4):545–559.

Xu, J., R.L. Dodd, C.L. Makino, M.I. Simon, D.A. Baylor, and J. Chen. 1997. Prolonged photoresponses in transgenic mouse rods lacking arrestin. *Nature*. 389:505–509.

Yau, K.-W. 1994. Cyclic nucleotide-gated channels: an expanding new family of ion channels. *Proc. Natl. Acad. Sci. USA*. 91:3481–3483.

Yokoyama, R., and S. Yokoyama. 2000. Comparative molecular biology of visual pigments. *In* Molecular Mechanisms in Visual Transduction. D.G. Stavenga, W.J. de Grip, and E.N. Pugh Jr., editors. Elsevier Science Publishing Co. Inc., New York. 257–296.

Yokoyama, S., F.B. Radlwimmer, and S. Kawamura. 1998. Regeneration of ultraviolet pigments of vertebrates. *FEBS Lett*. 423:155–158.

Yoshida, S., A.J. Mears, J.S. Friedman, T. Carter, S. He, E. Oh, Y. Jing, R. Farjo, G. Fleury, C. Barlow, et al. 2004. Expression profiling of the developing and mature *Nrl*$^{-/-}$ mouse retina: identification of retinal disease candidates and transcriptional regulatory targets of Nrl. *Hum. Mol. Genet*. 13:1487–1503.

Zhu, X., B. Brown, A. Li, A.J. Mears, A. Swaroop, and C.M. Craft. 2003. GRK1-dependent phosphorylation of S- and M-opsins and their binding to cone arrestin during cone phototransduction in the mouse retina. *J. Neurosci*. 23:6152–6160.